The Abdus Salam International Centre for Theoretical Physics

2132-34

Winter College on Optics and Energy

8 - 19 February 2010

Femtosecond laser micromachining

R. Ramponi
Politecnico di Milano
Milano
Italy

POLITECNICO DI MILANO

Femtosecond laser micromachining

Roberta Ramponi

Politecnico di Milano – Department of Physics & IFN-CNR

roberta.ramponi@fisi.polimi.it

Outline of the presentation

- Nonlinear light-matter interaction, photoinduced material modifications
- Femtosecond laser optical waveguide writing
- Fabrication of integrated photonic devices
  - passive devices
  - active devices
- Femtosecond laser microstructuring for optofluidics
  - microfluidic channels by irradiation + etching
  - new optofluidic functionalities by waveguide-channel integration
- Femtosecond laser microstructuring for solar cells

Material modification following nonlinear light absorption

Multiphoton ionization

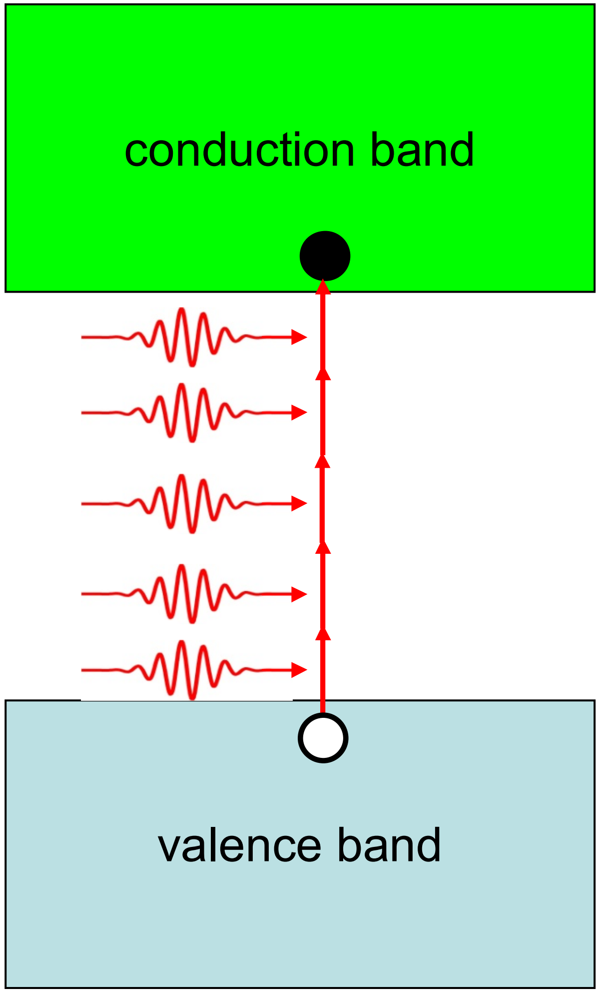

- Simultaneous absorption of k photons brings electron from valence to conduction band

$$\frac{dn}{dt} = \sigma_k I^k(t)$$

n(t) electron density
I(t) laser intensity
σ_k k-photon absorption cross section

Avalanche ionization

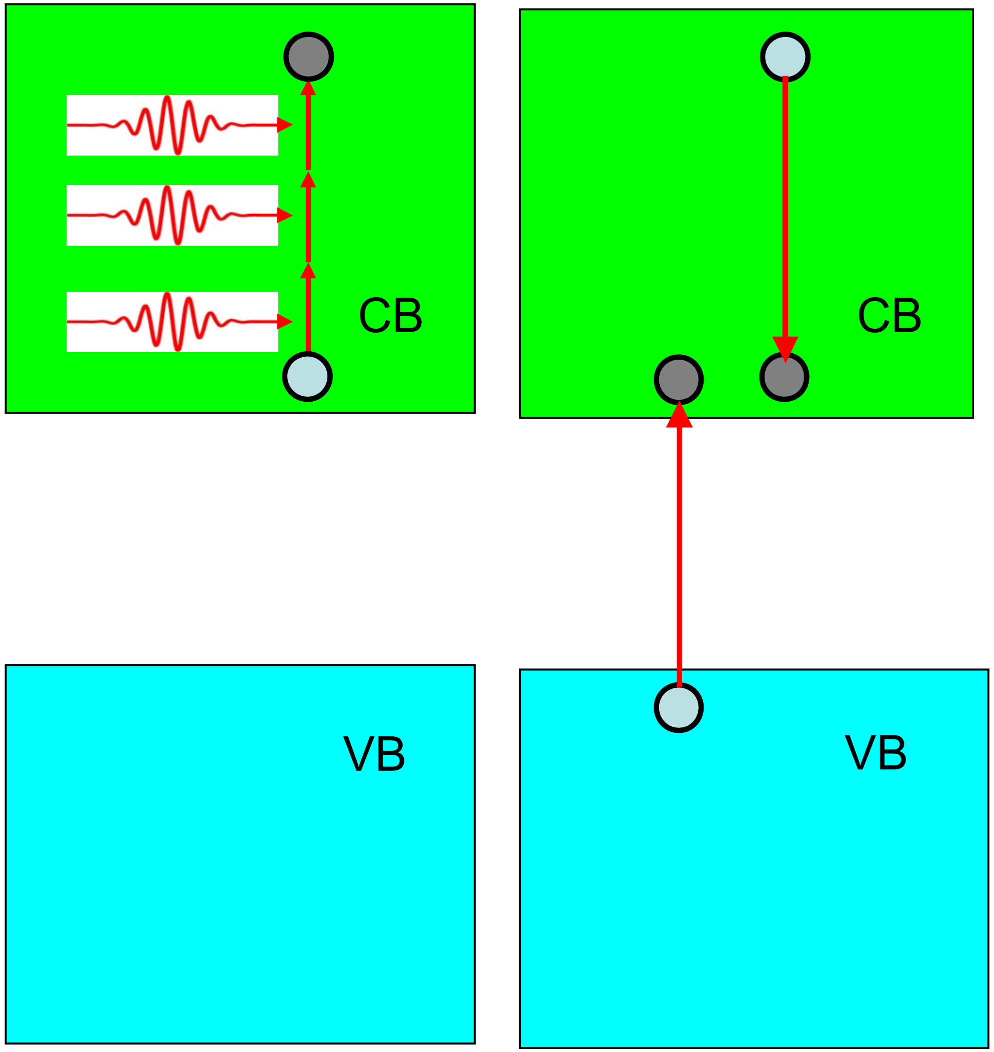

- Free electrons in the conduction band are accelerated by the laser field until they have enough kinetic energy to kick another electron into the conduction band

$$\frac{dn}{dt} = \alpha I(t) n(t)$$

α avalanche ionization coefficient

Femtosecond vs long-pulse absorption

Femtosecond absorption

- The peak power is sufficient to trigger, in the focus, **multiphoton ionization** which provides a **seed of electrons** in the conduction band

- The electrons are accelerated by the laser and **multiplied by avalanche ionization** ⇒ **deterministic** and highly reproducible process

Long pulse absorption

- The peak power is too low for **multiphoton ionization**

- Avalanche ionization initiated by spurious free electrons in the conduction band from defects or impurities ⇒ **poorly reproducible** process

Femtosecond vs long-pulse absorption

Femtosecond absorption

- The peak power is sufficient to trigger, in the focus, **multiphoton ionization** which provides a **seed of electrons** in the conduction band

- The electrons are accelerated by the laser and **multiplied by avalanche ionization** ⇒ **deterministic** and highly reproducible process

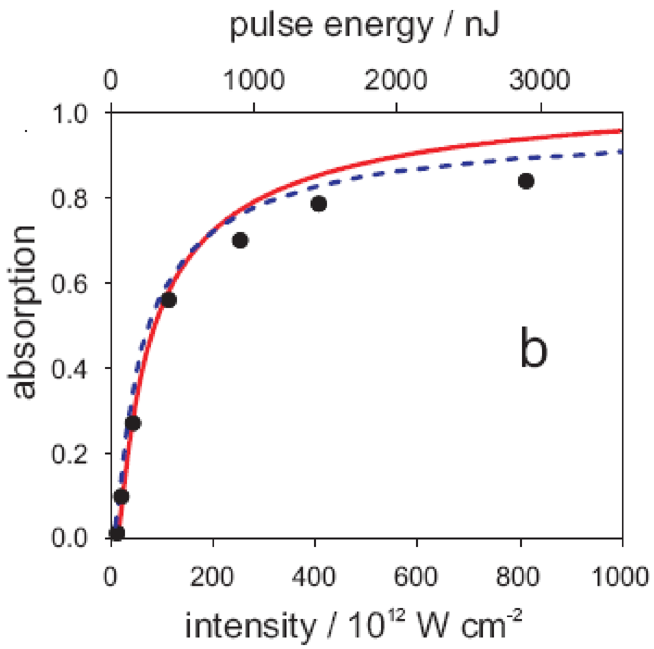

Femtosecond pulse absorption as a function of peak intensity (Rayner *et al.*, Opt. Express **13**, 3208 (2005))

Highly localized and reproducible deposition of energy in the focus of the laser beam

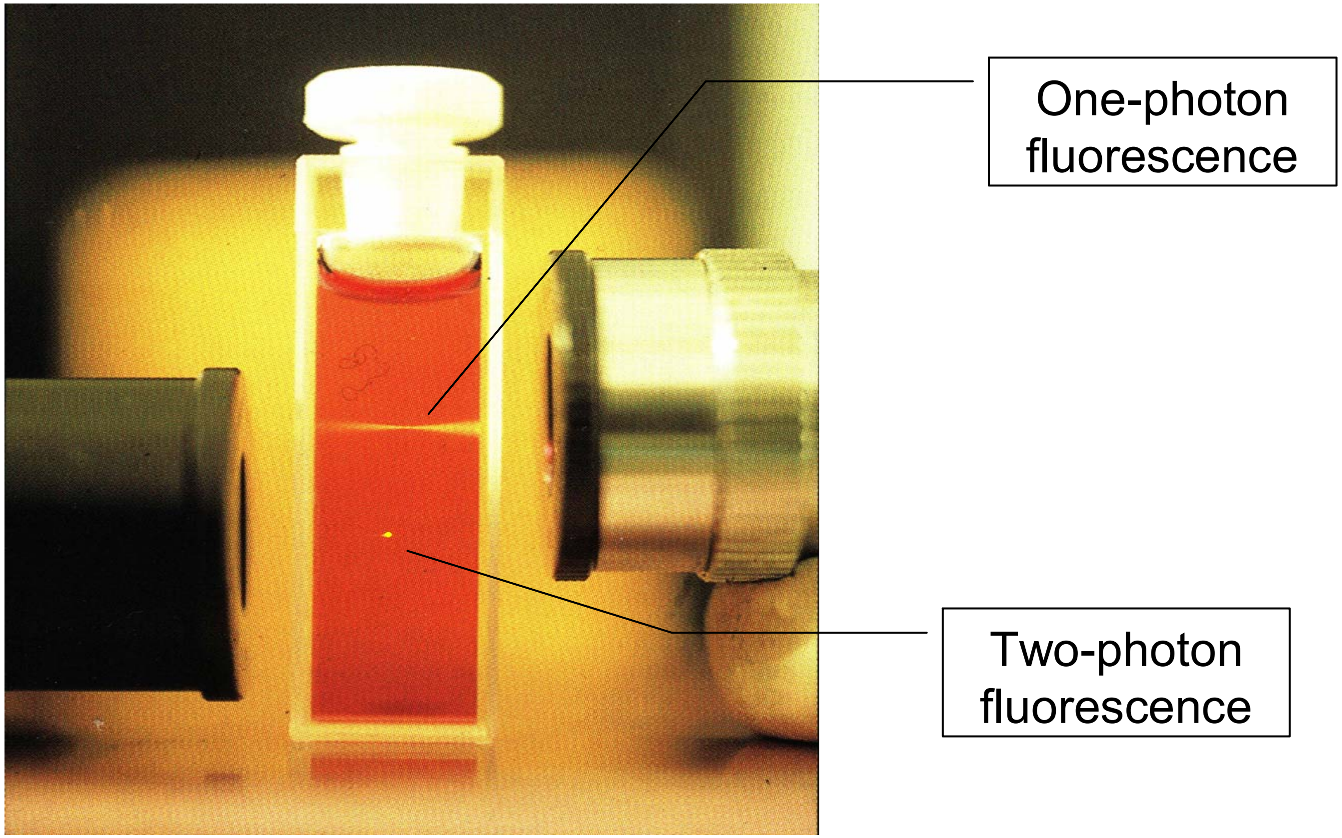

Light is absorbed only in the focus, where the intensity is sufficient

W. Denk et al., Science **248**, 73 (1990)

What happens following nonlinear light absorption?

Timescales of light-matter interaction in transparent materials

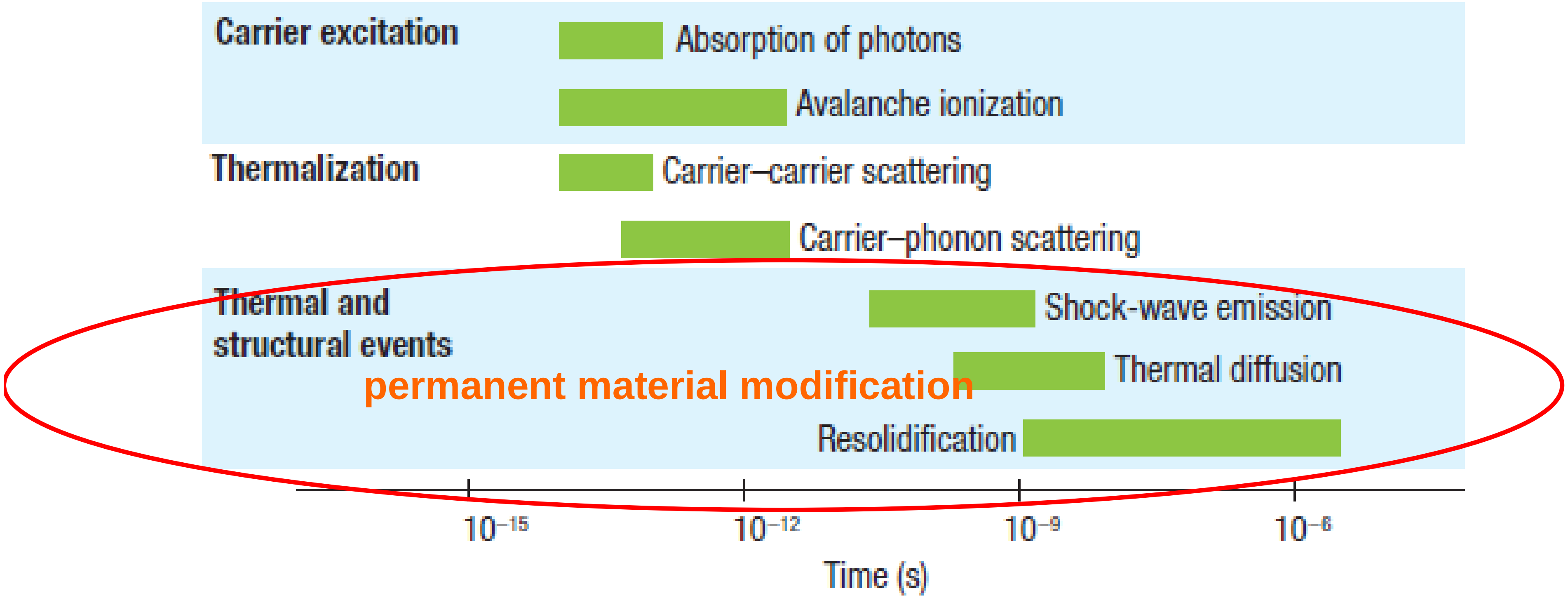

R. Gatass and E. Mazur, Nature Photonics **2**, 219 (2008)

Regimes of material modification

waveguide writing

"gentle" modification
refractive index change

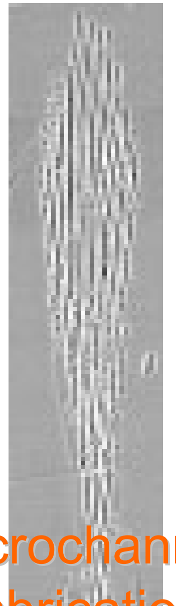

microchannel fabrication

formation of nanogratings

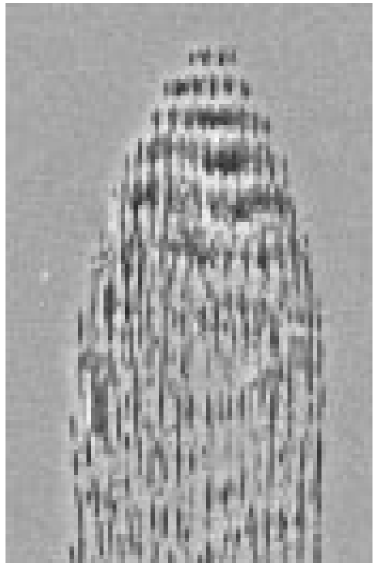

disruptive changes

Increasing laser fluence →

R. Taylor et al., Laser Photonics Reviews **2**, 26 (2008)

Femtosecond laser

optical waveguide writing

Femtosecond laser waveguide writing

November 1, 1996 / Vol. 21, No. 21 / OPTICS LETTERS 1729

Writing waveguides in glass with a femtosecond laser

K. M. Davis, K. Miura, N. Sugimoto, and K. Hirao

Hirao Active Glass Project, Exploratory Research for Advanced Technology, Research Development Corporation of Japan, 15 Mori Moto-Cho, Shimogamo, Sakyo-Ku, Kyoto G06, Japan

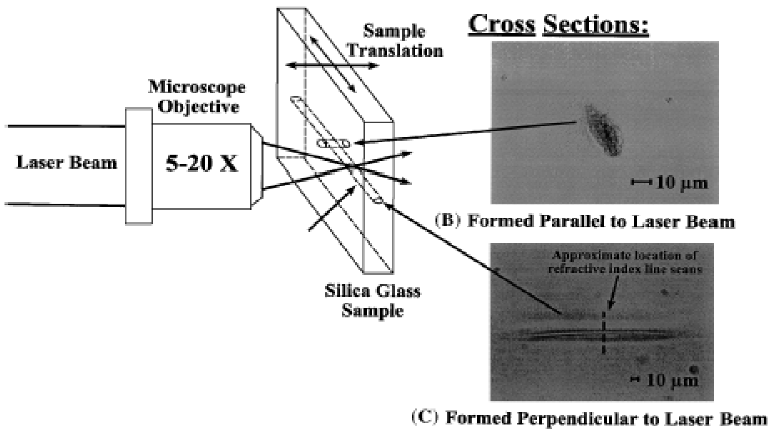

Seminal paper by Hirao et al., demonstrating permanent positive refractive index changes

Origins of refactive index change

Not yet fully understood, several mechanisms have been proposed such as:

- **Structural modifications**, i.e. changes in the structure of the glass network

- **Color center formation**, with UV absorption causing a refractive index change through Kramers-Krönig

- **Melting and rapid resolidification (quenching),** causing regions of material densification

These mechanisms may act simultaneously.

A.M. Streltsov et al., J. Opt. Soc. Am. B **19,** 2496 (2002)

Femtosecond laser waveguide writing

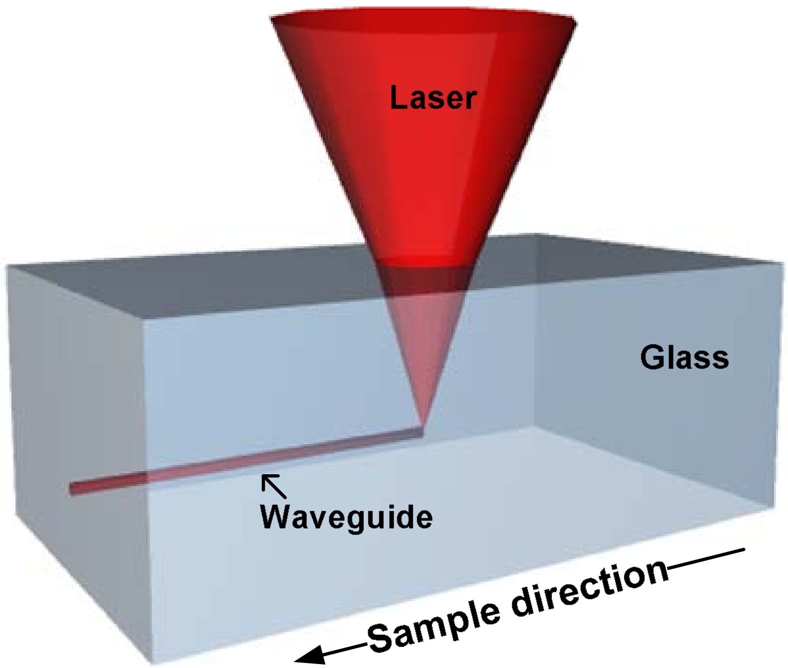

Advantages:

- Direct fabrication technique, no need for clean rooms and photolithography
- Maskless technique, suitable for rapid prototyping
- Applicable to a wide variety of substrates, both amorphous and crystalline
- 3D device fabrication capabilities

Waveguide fabrication setup

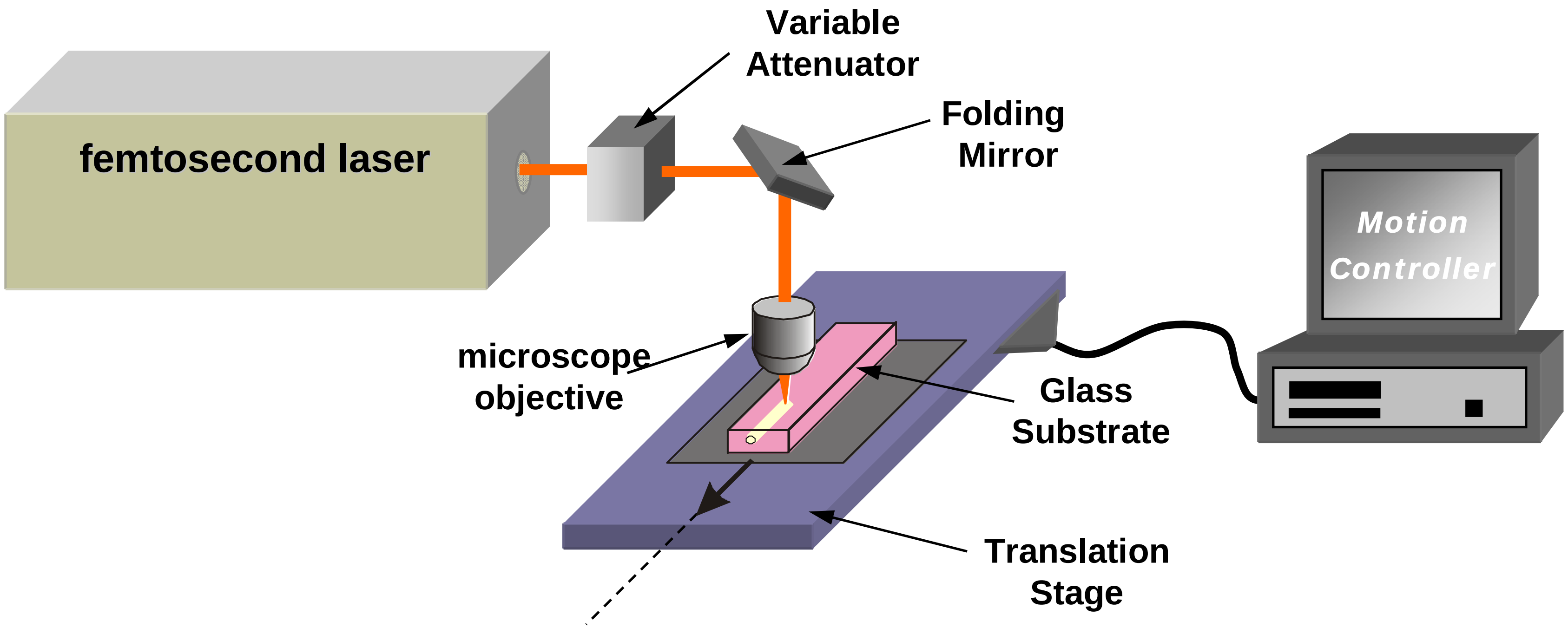

- The basic setup is remarkably simple: laser, focusing optics, computer-controlled translation stage

Lasers used in waveguide fabrication

- **Amplified Ti:Sapphire systems:** 100-200 fs long pulses at 800nm, few μJ energies per pulse, 1-200 kHz repetition rate

single-pulse regime

- **Diode-pumped fiber or bulk Yb lasers:** 300-400 fs long pulses at 1040nm, < 1 μJ energies per pulse,200 kHz-2 MHz repetiton rate

cumulative regime

- **Long-cavity Ti:Sapphire oscillators:** 10-50 fs long pulses at 800nm, tens of nJ energy per pulse, 4-25 MHz repetition rate

Cumulative regime: pulse period much shorter than heat diffusion time out of the focal volume

repetition rate

Single-pulse regime: the asymmetry problem

- In transverse geometry, writing with low repetition rate systems provides waveguides with an intrinsically asymmetric cross section → very poor coupling with standard fibers

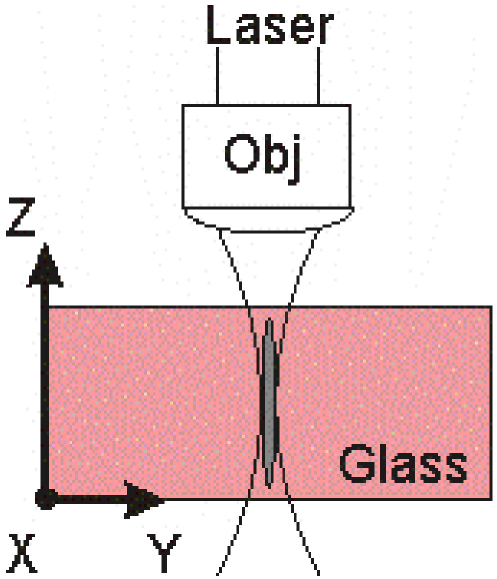

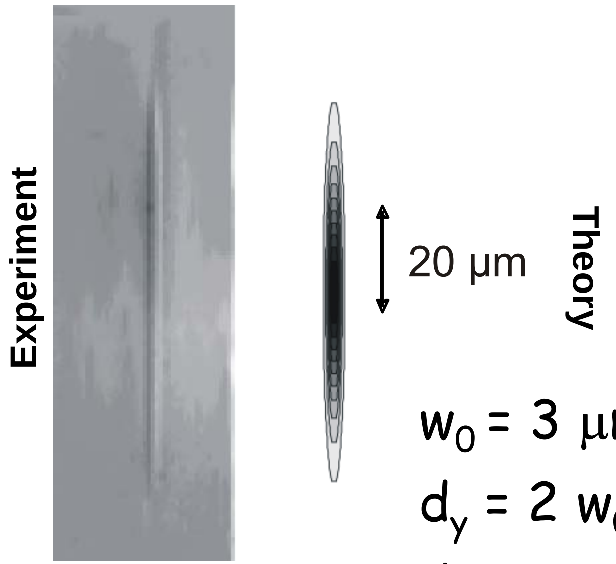

$w_0 = 3\ \mu m$

$d_y = 2\ w_0 = 6\ \mu m$

$d_z = 2\pi w_0^2/\lambda = 72\ \mu m$

- The confocal parameter is much larger than the focal diameter

Solution: astigmatic beam shaping

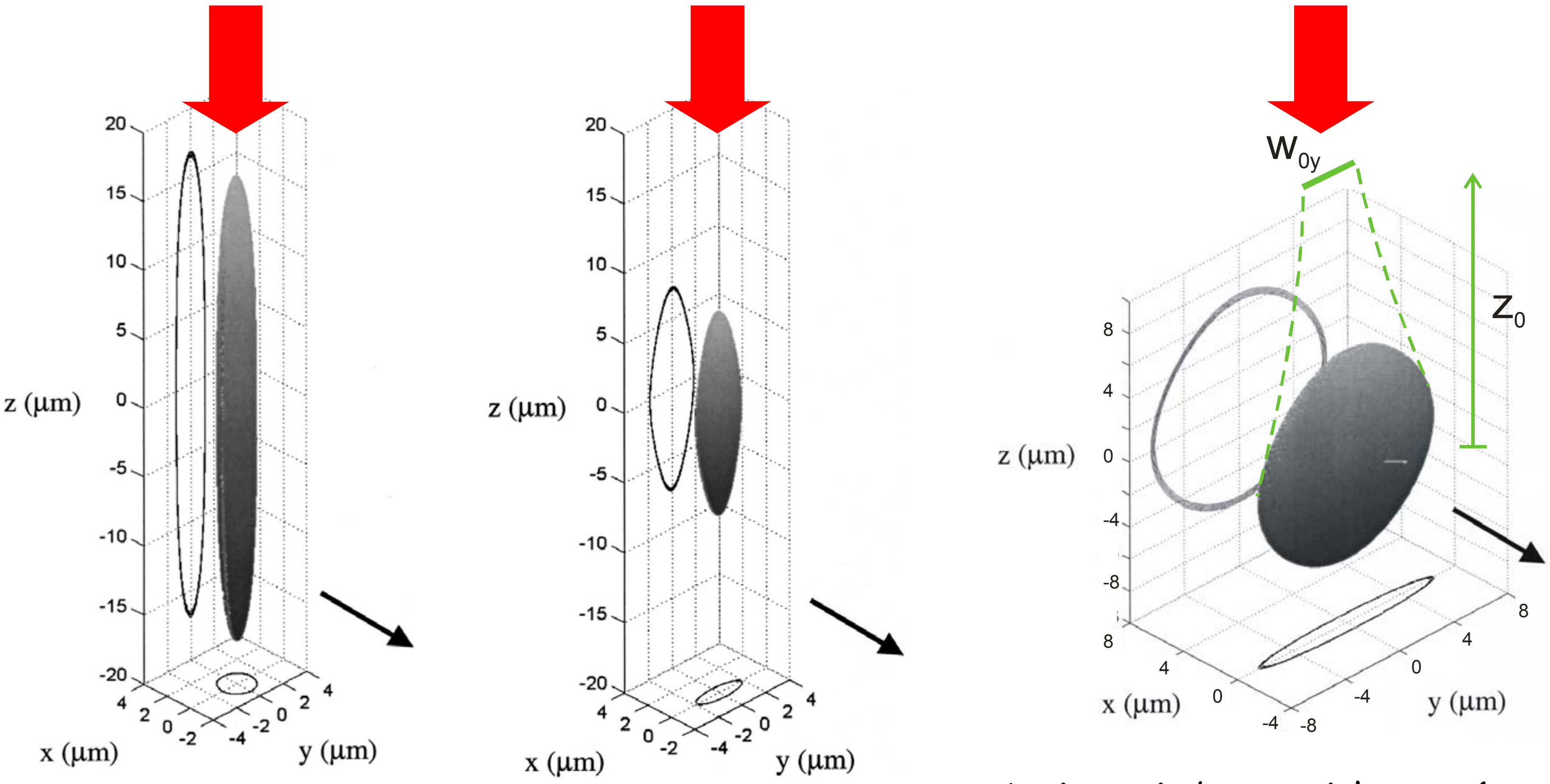

Standard beam with w_0= 2μm

Astigmatic beam with w_{0x}= 1μm and w_{0y}=3μm

Astigmatic beam with w_{0x}= 1μm and w_{0y}=3μm, but with an offset of z_0=180μm

G. Cerullo *et al.*, Optics Letters **27**, 1938 (2002)

Astigmatic beam shaping: experimental results

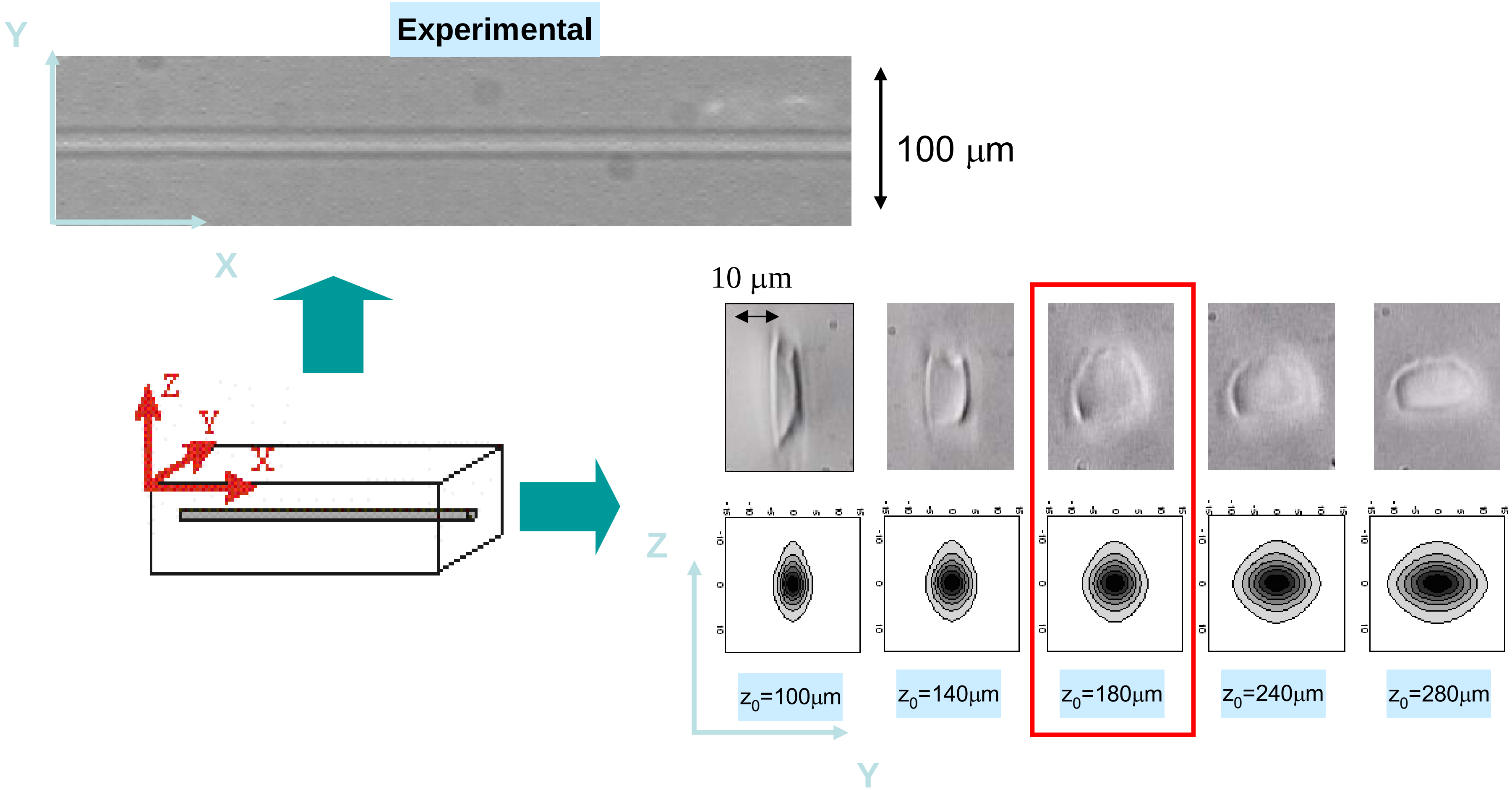

R. Osellame *et al.*, J. Opt. Soc. Am. B **20**, 1559 (2003)

Other beam shaping techniques

- Slit Beam shaping

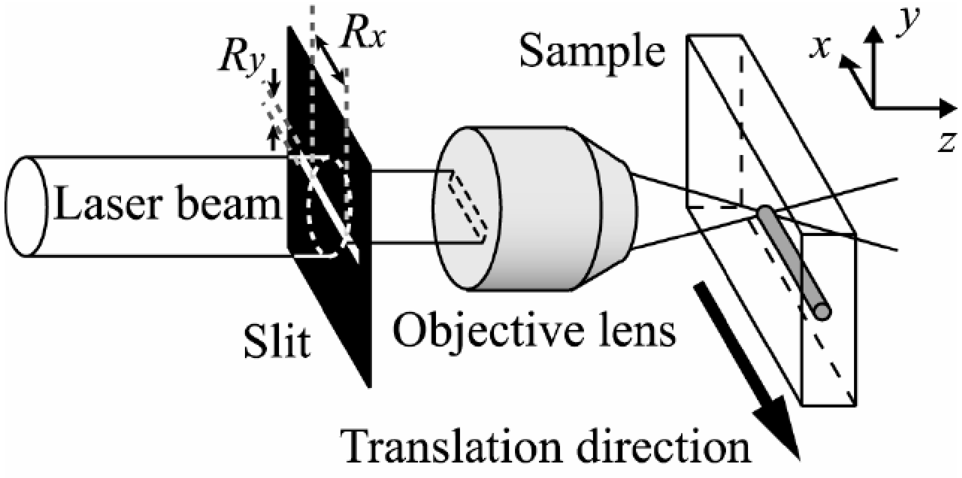

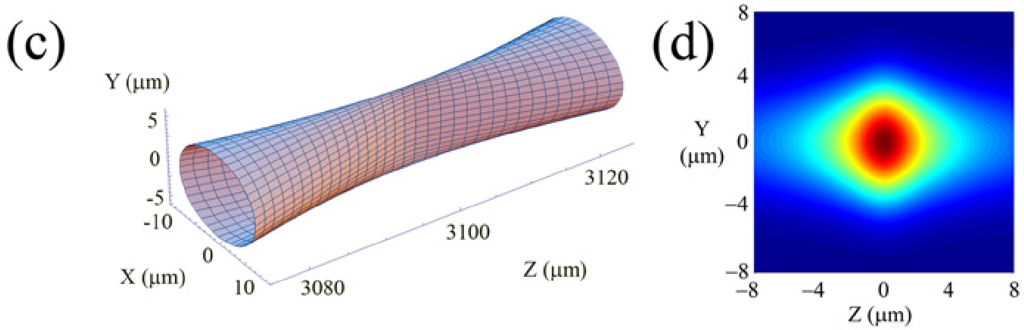

S. Sowa *et al.*, Opt. Expr. **14**, 291 (2006)

- Multiscan approach

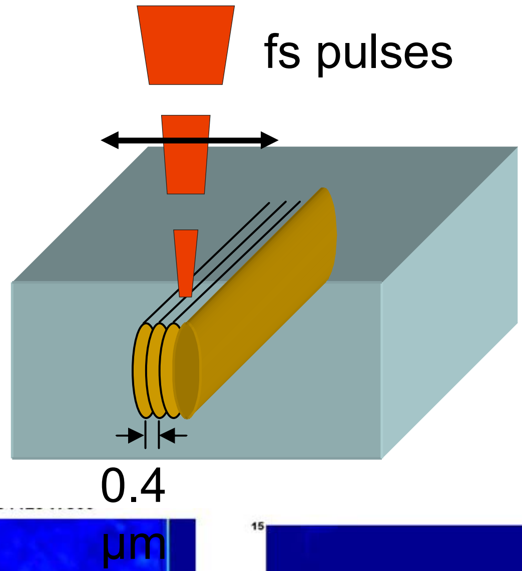

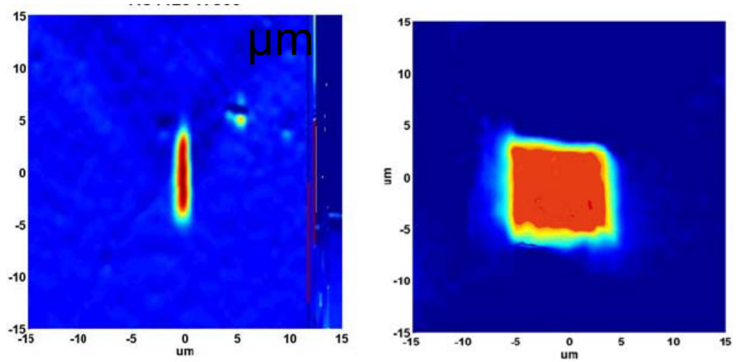

Y. Nasu *et al.*, Opt. Lett. **30**, 723 (2005)

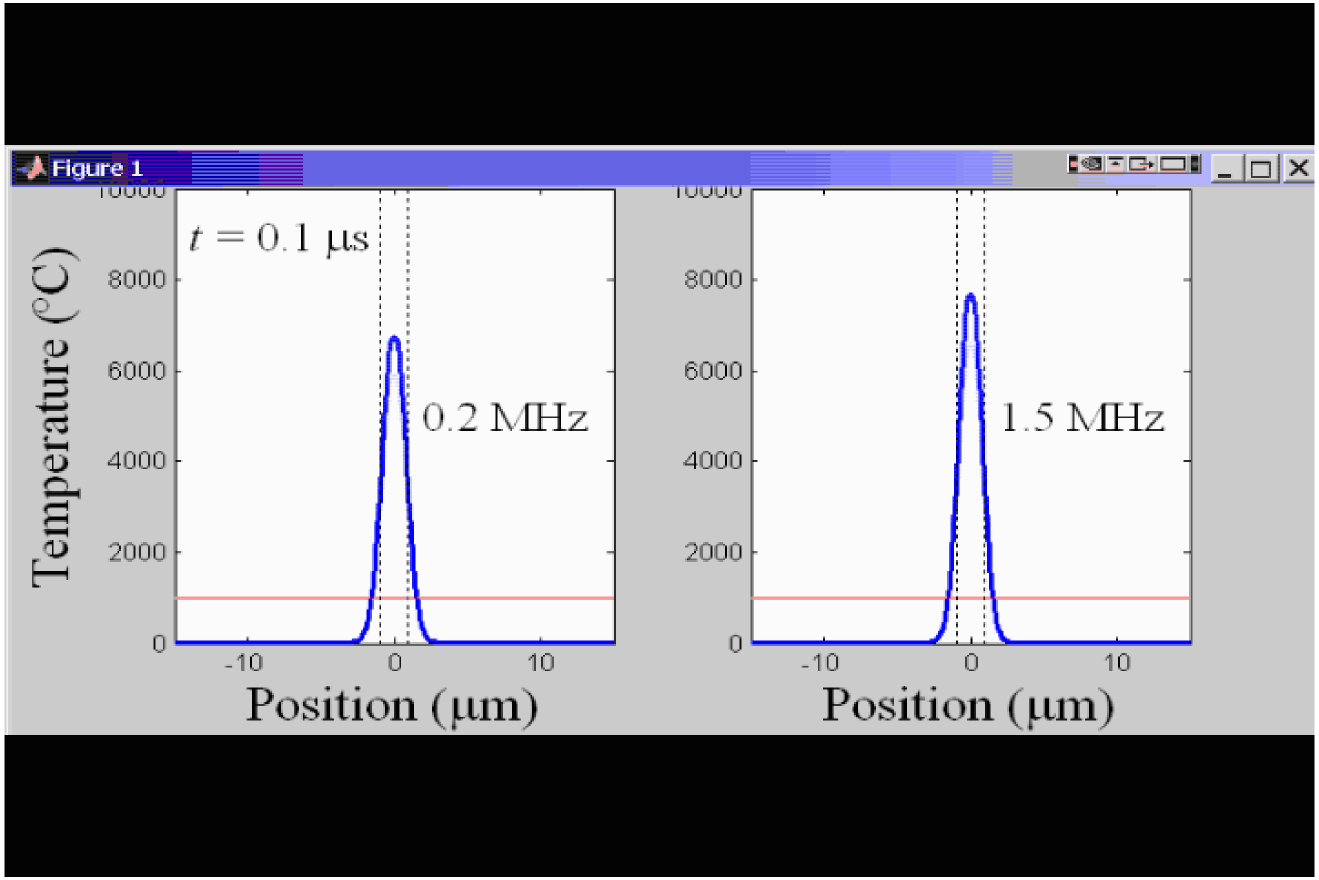

- Borosilicate glass. Heat diffusion time out of focal volume ~1 μs

S. Eaton et al., Opt. Express **16**, 9443 (2008)

Waveguide writing in the cumulative regime

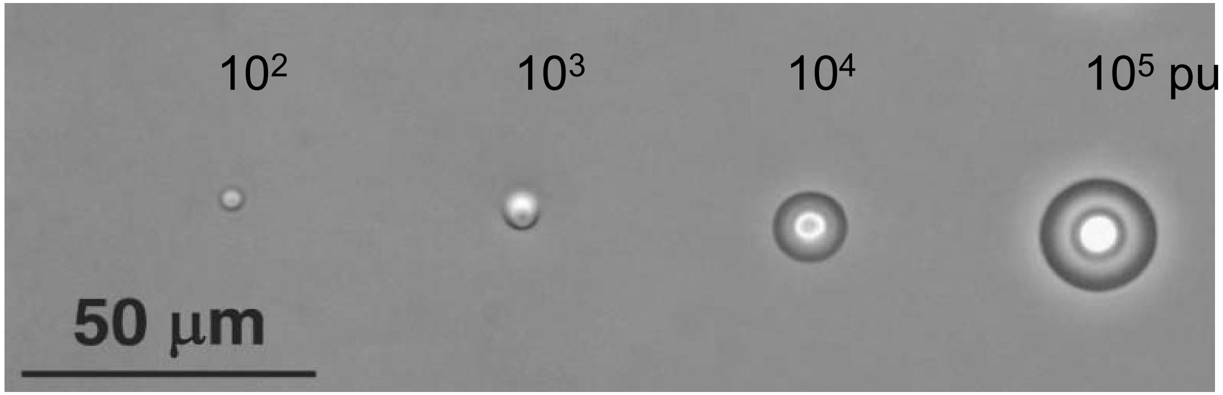

- Due to isotropic heat diffusion, waveguide cross section becomes symmetric

- Waveguide cross-section can be controlled by average power and translation speed

S. Eaton et al., Opt. Express **13**, 4708 (2005)

C. Schaffer et al., Appl. Phys. A **76**, 351 (2003)

Passive photonic devices by femtosecond writing

Waveguides mode matched to telecom fibers

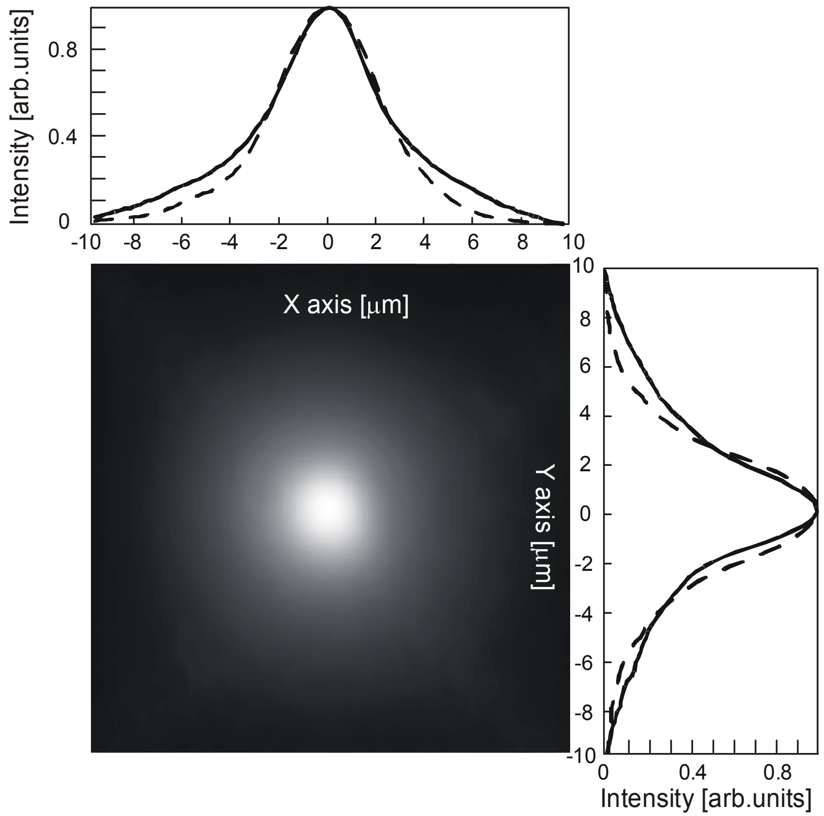

- Single transverse mode waveguides with high circular symmetry at 1.5 μm.

- Mode matching with standard telecom fibers: 0.2 dB coupling losses (propagation losses < 0.2 dB/cm)

- Splitter

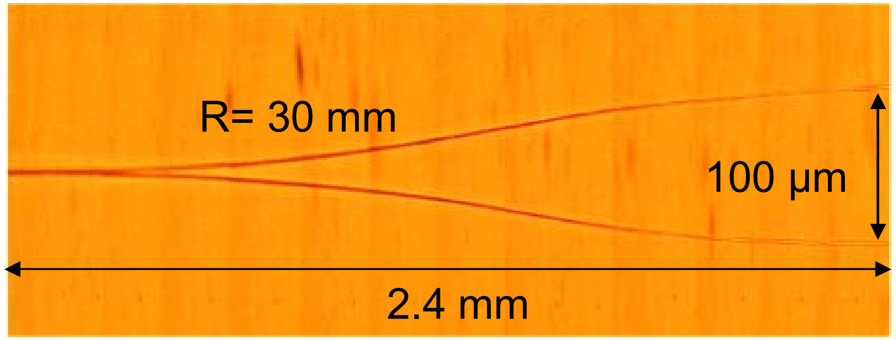

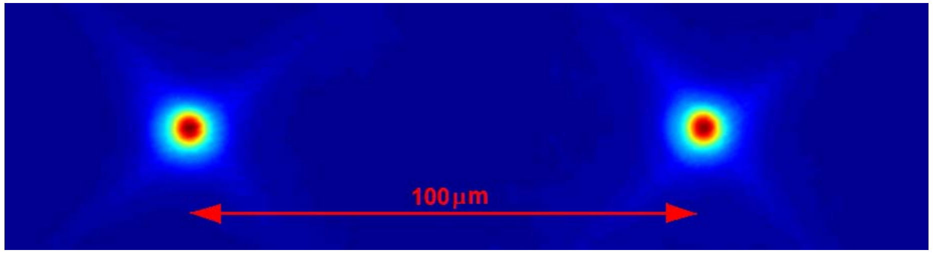

- Directional coupler

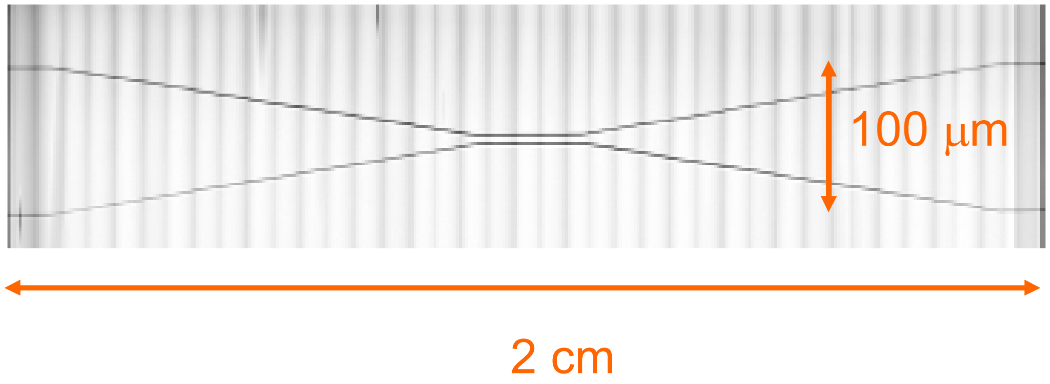

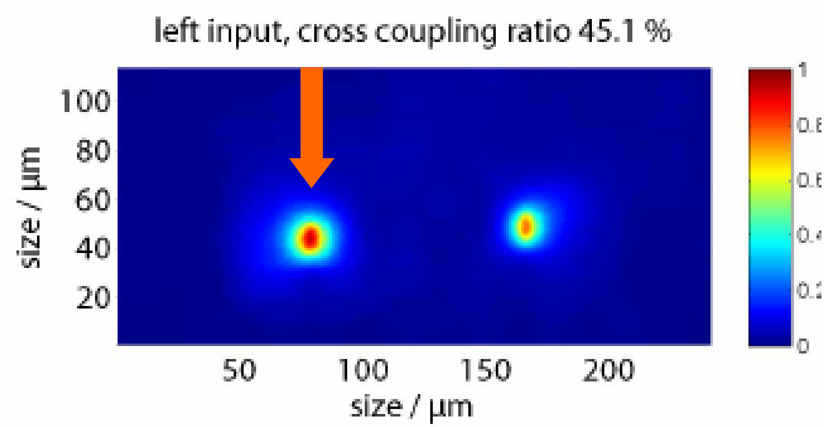

Bragg grating waveguide fabrication: single pulse method

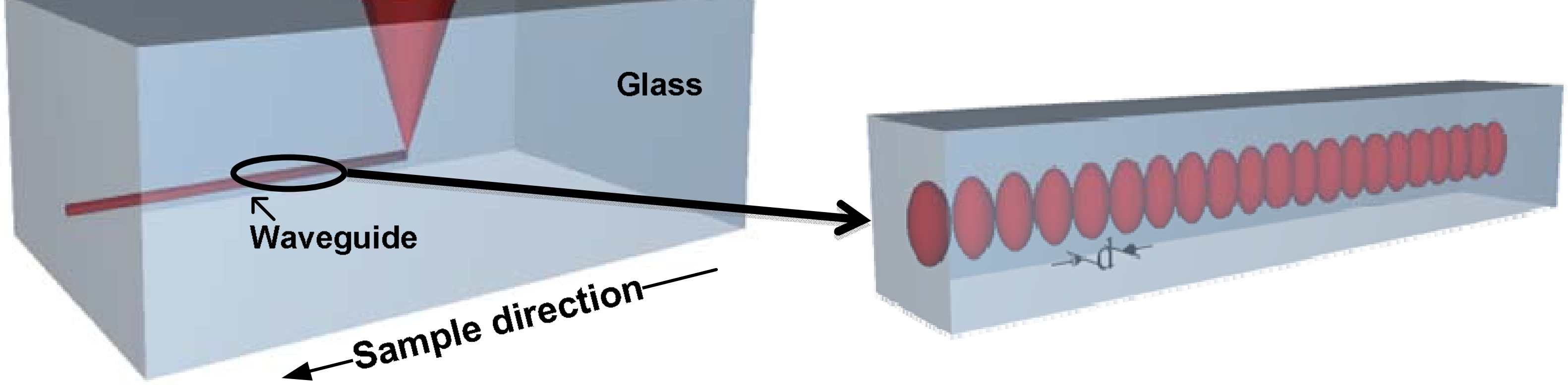

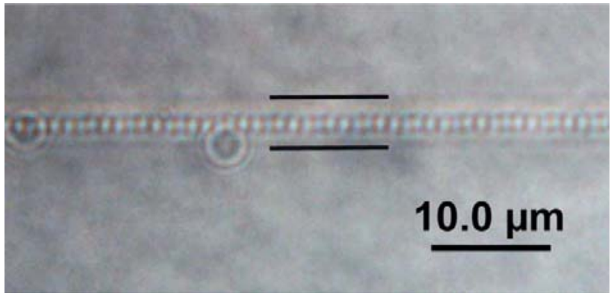

- Laser is scanned rapidly, so individual shots create periodic index modulation

G.D Marshall et al., Opt. Lett. **31**, 2690 (2006)

H. Zhang et al., Opt. Lett. **31**, 3495 (2006)

Bragg grating waveguide fabrication: burst method

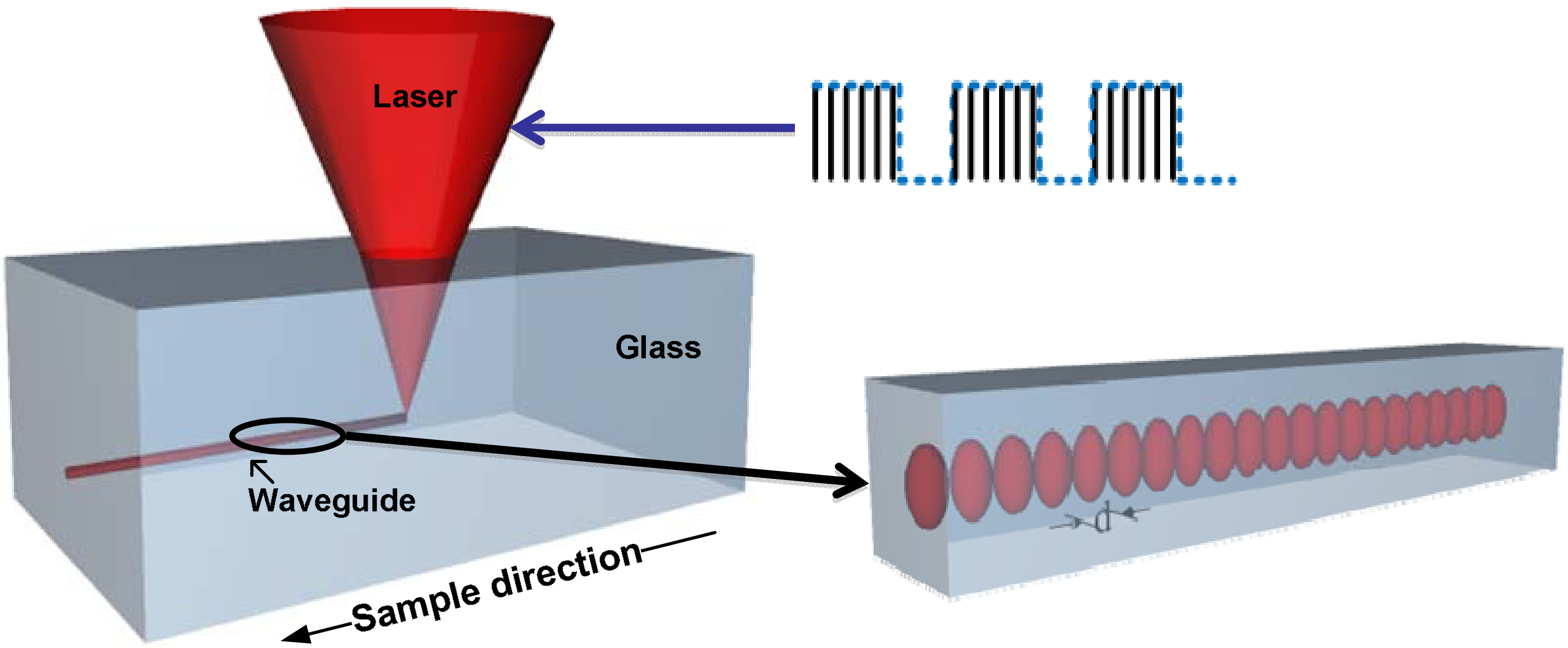

- Writing beam intensity periodically modulated by acousto-optic modulator

H. Zhang *et al.*, Opt. Lett. **32**, 2559 (2007)

Bragg grating waveguides performance

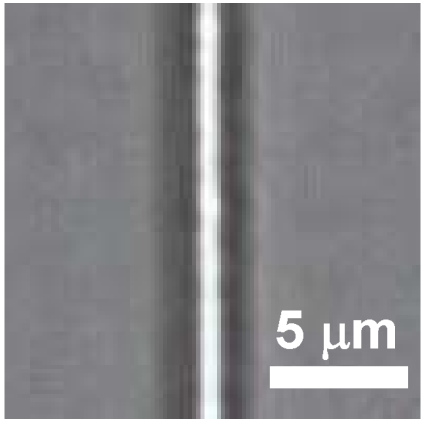

60%

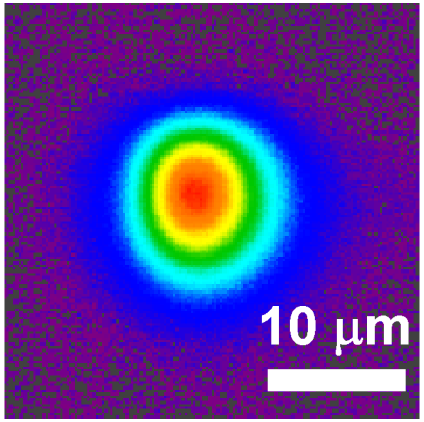

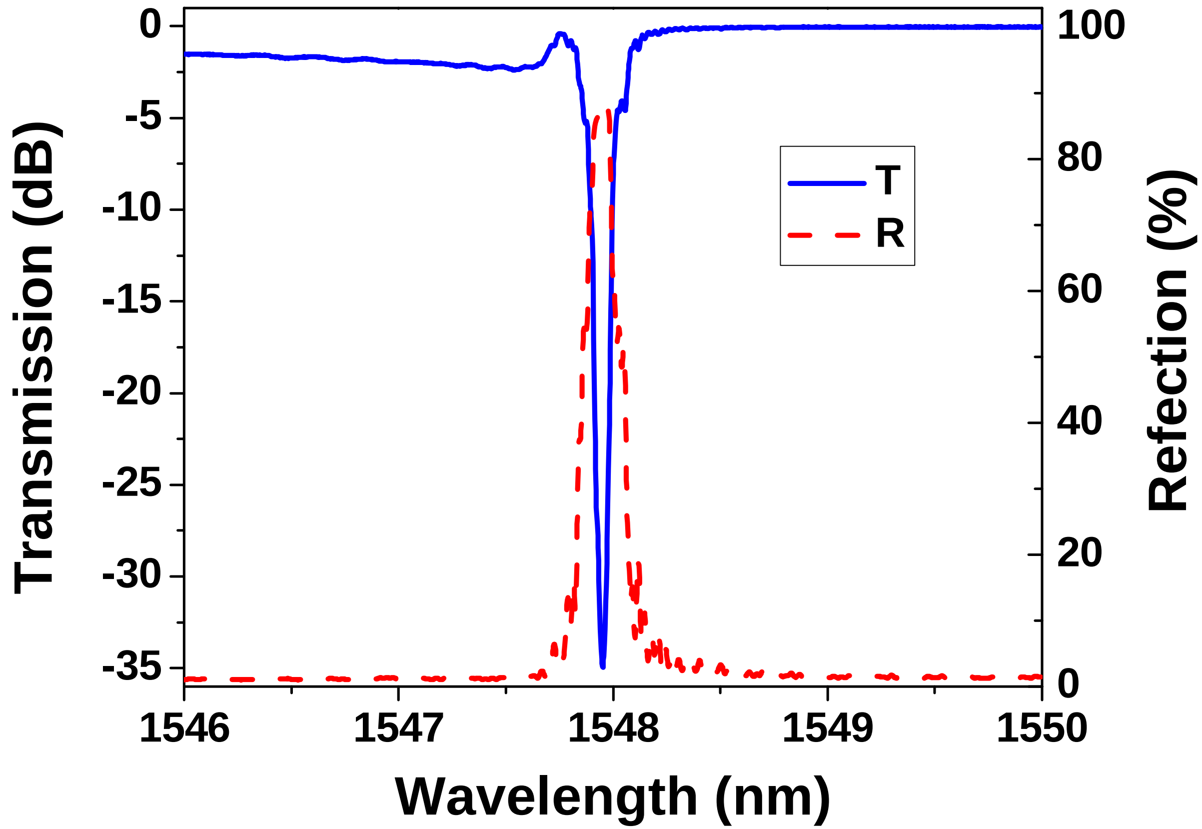

H. Zhang *et al.*, Opt. Lett. **32**, 2559 (2007)

Three-dimensional writing capabilities

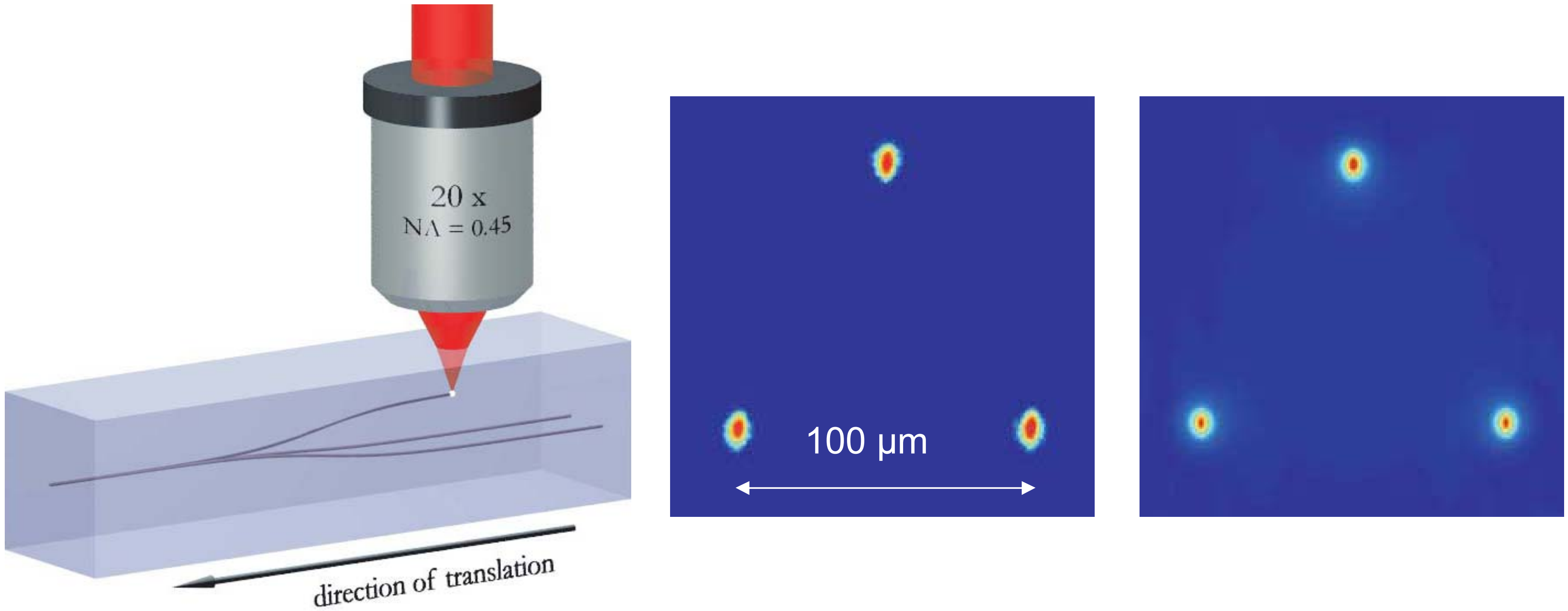

- Three-dimensional splitter written in fused silica

S. Nolte et al., Appl. Phys. A **77**, 109 (2003)

- Three-waveguide directional coupler

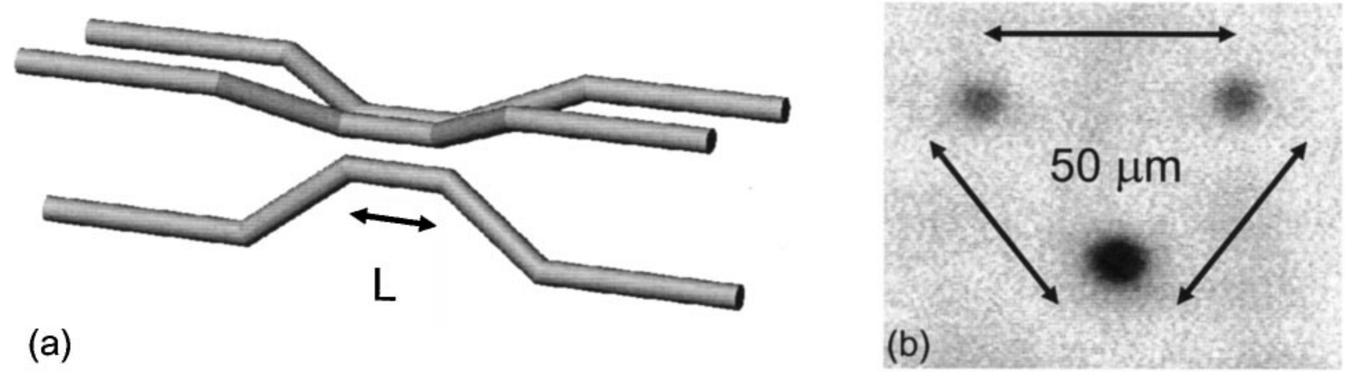

- 3D microring resonator

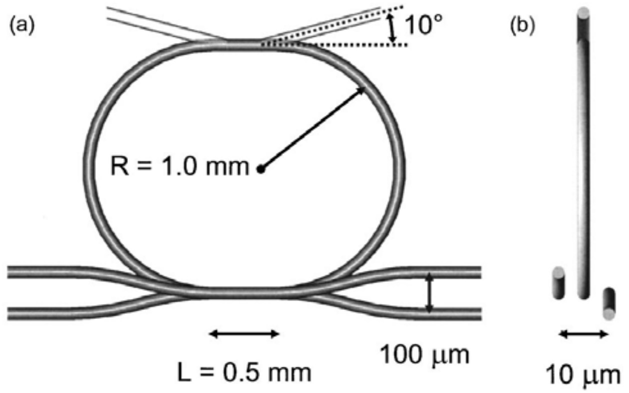

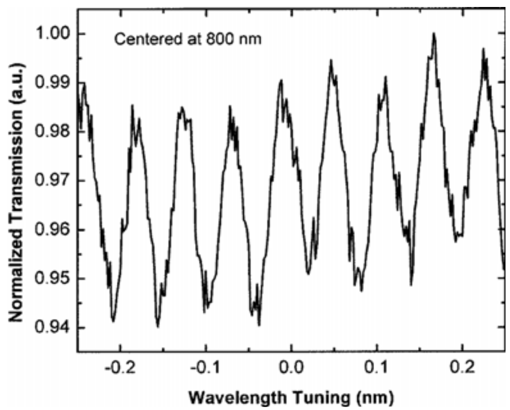

A. M. Kowalevicz *et al.*, Opt. Lett. **30**, 1060 (2005)

Active photonic devices
by femtosecond writing

Substrate material: Er:Yb-doped phosphate glass

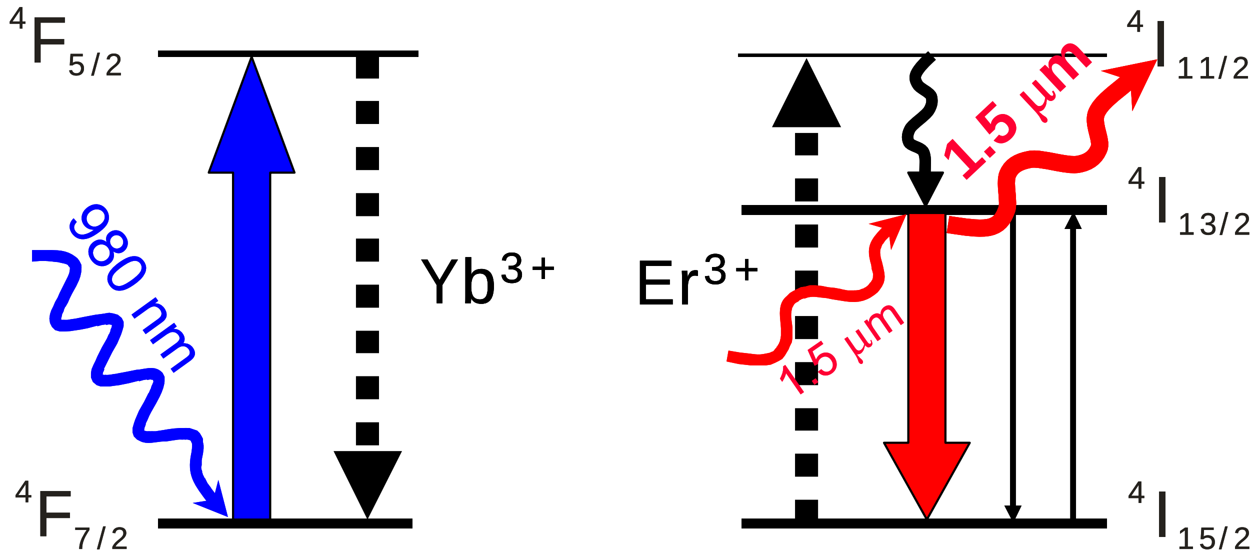

- Glass base suitable for compact active devices (high-gain per unit length)
- Allows for high doping concentration: 1-10 % weight Er_2O_3 or Yb_2O_3
- Three-level system, pumped at 980 nm and lasing at 1.5 μm in the telecom band

Active waveguides with net gain in the whole telecom C-band

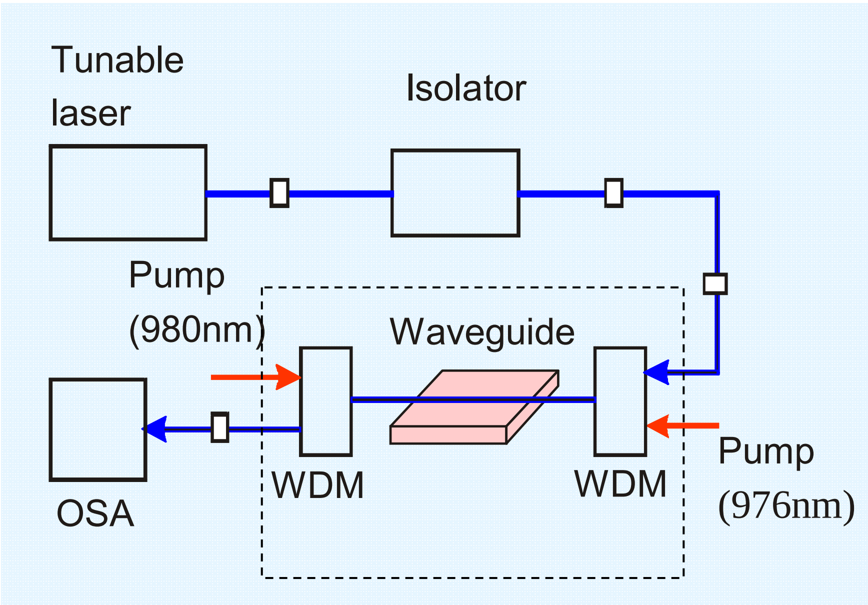

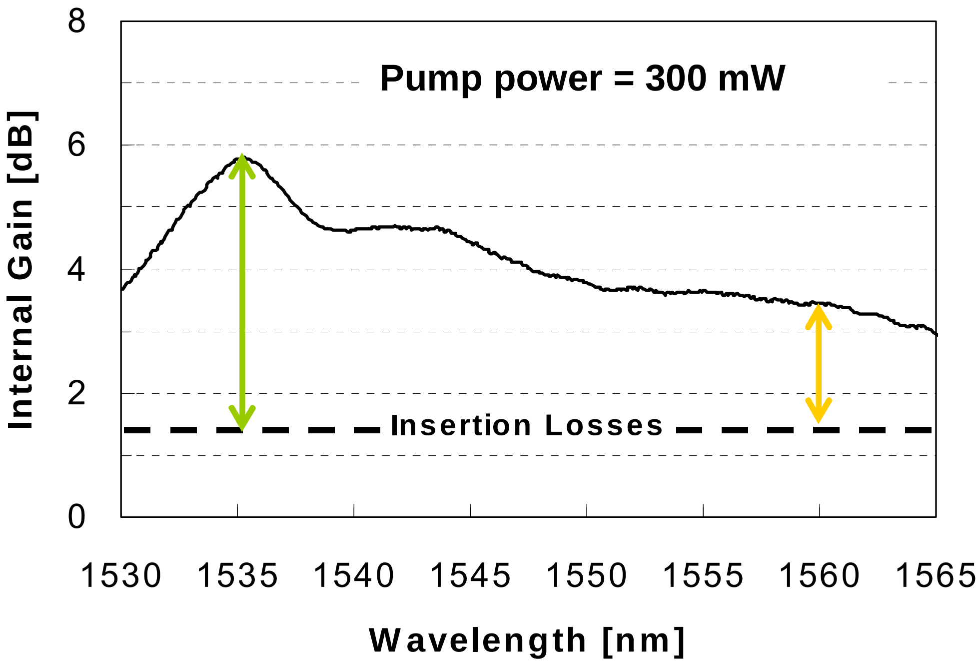

- Internal gain (6 dB) overcomes insertion losses (1.4 dB) over the whole C band
- Possibility of active devices such as waveguide amplifiers or lasers

R. Osellame *et al.*, Opt. Lett. **29**, 1902 (2004)

Femtosecond laser written Erbium-Doped Waveguide Amplifier

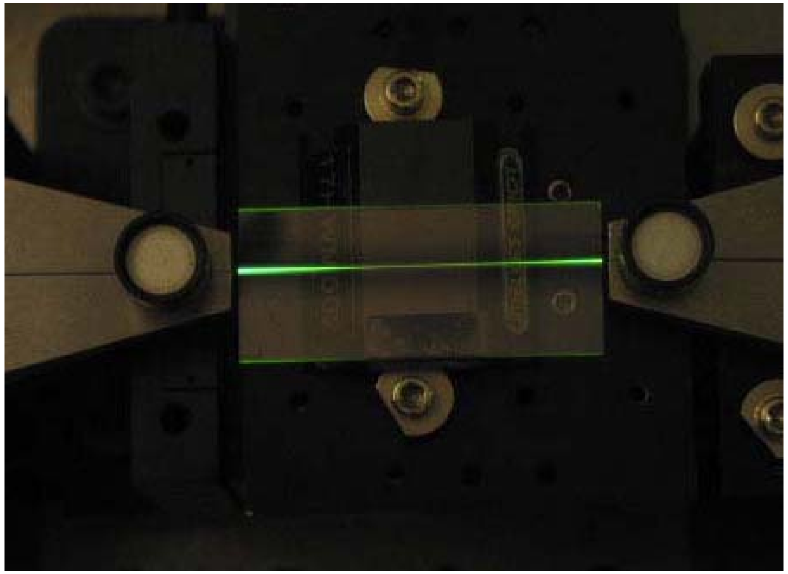

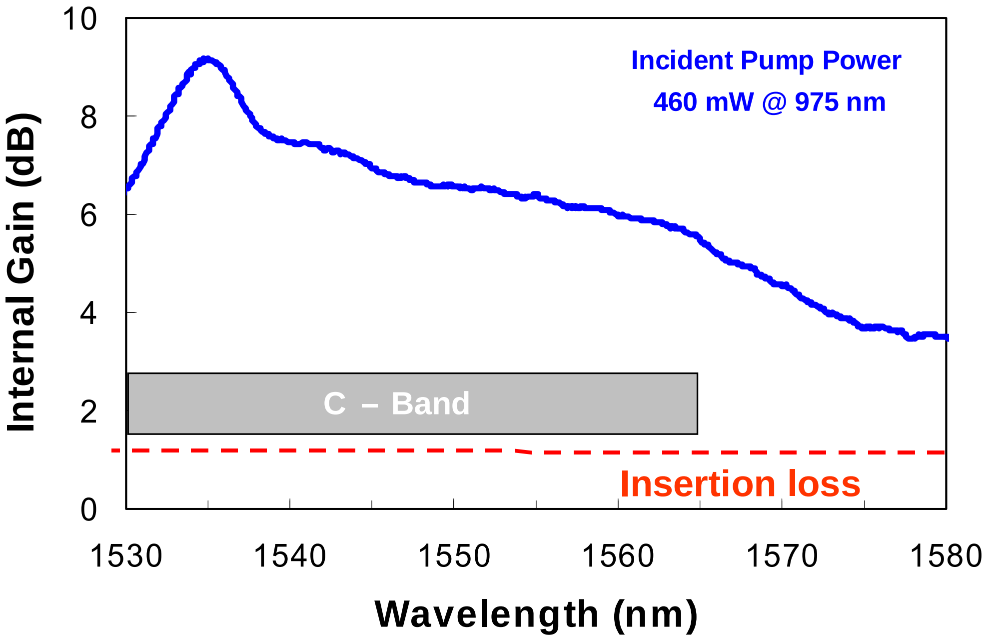

- Improved insertion losses (1.9 dB for L=37 mm → propagation loss < 0.4 dB/cm)
- Gain over the whole C-band: 7.4 dB peak at 1535 nm,3.7 dB at 1565 nm

G. Della Valle et al., Opt. Express **13**, 5976 (2005)

Femtosecond laser written waveguide laser

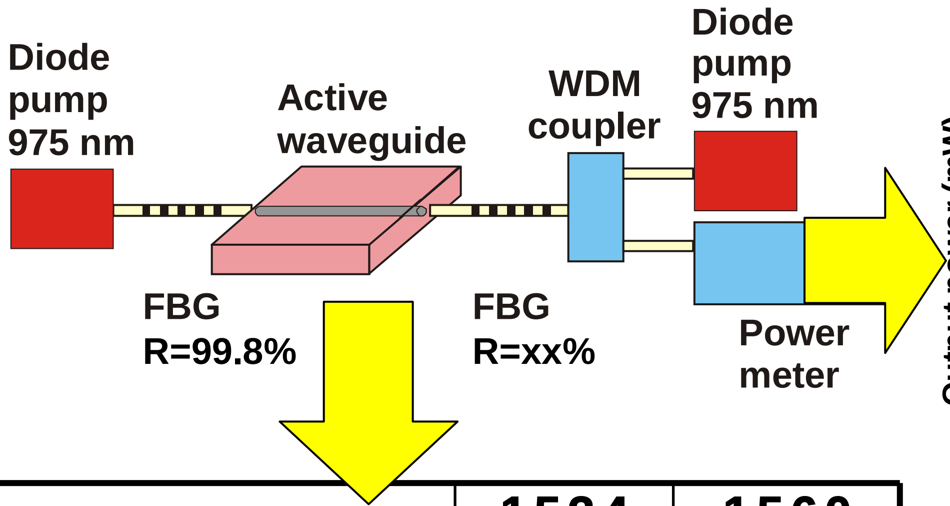

Performance	1534 nm	1560 nm
Pump Power Threshold (mW)	112	102
Maximum Output Power (mW)	32.3	19.2
Slope Efficiency	8.4 %	5.8 %

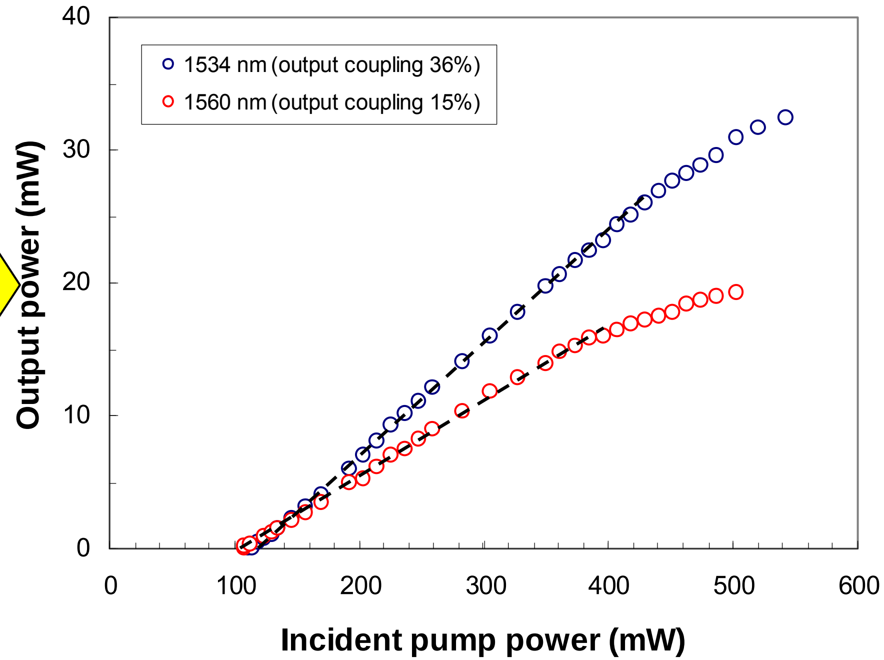

Waveguide laser array on the ITU grid

S. Taccheo *et al.*, Opt. Lett. **29**, 2626 (2004)

Single longitudinal mode waveguide laser

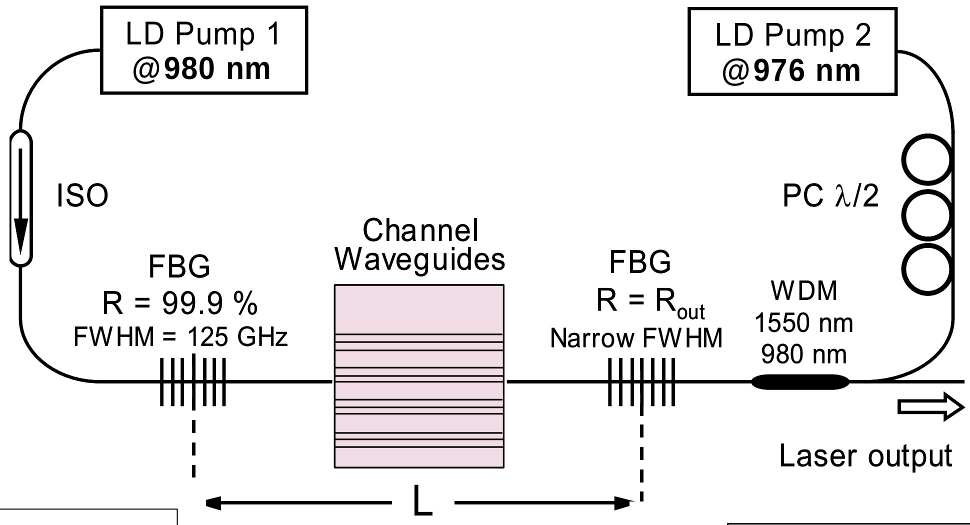

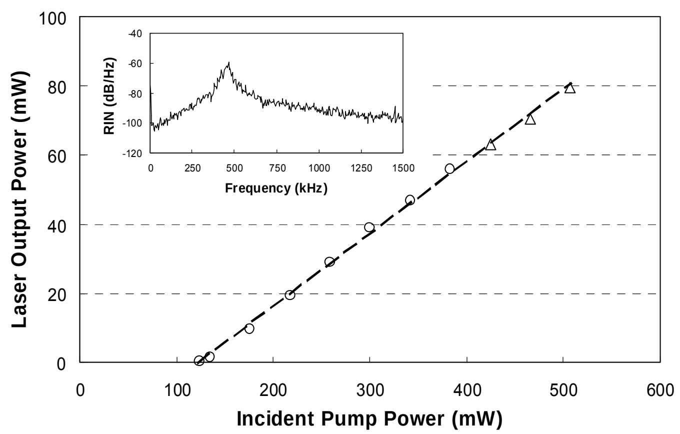

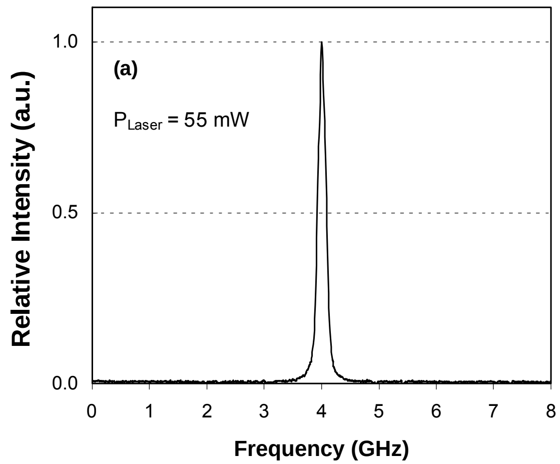

G. Della Valle *et al.*, Opt. Express **15**, 3190 (2007)

Waveguide laser with distributed feedback Bragg grating

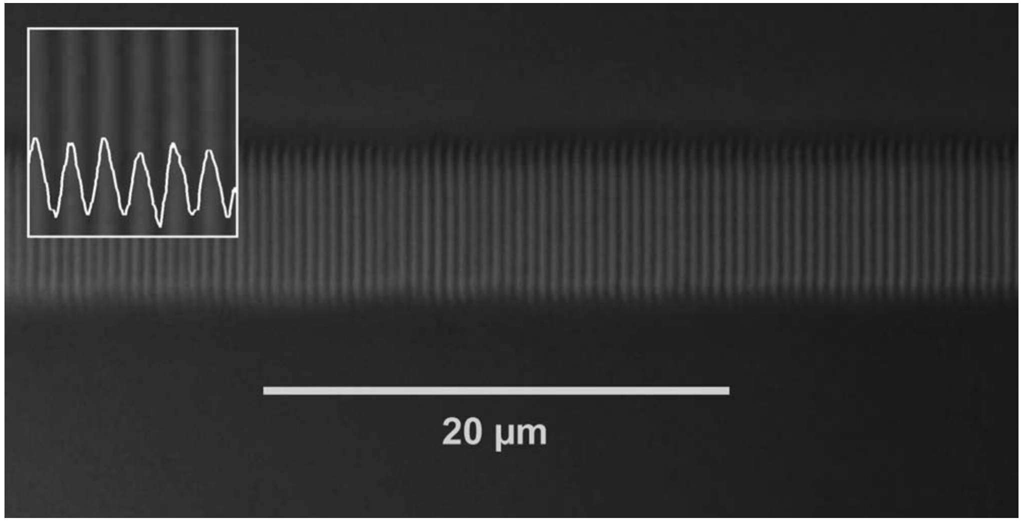

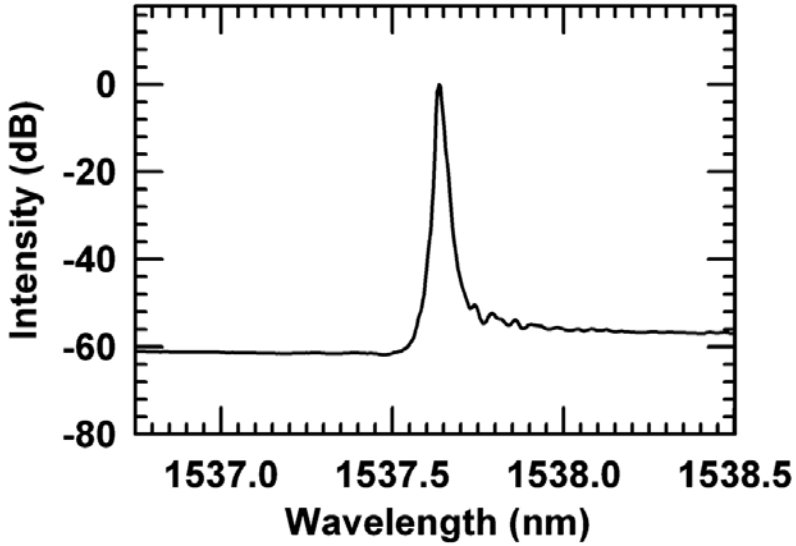

- Femtosecond laser written Bragg gratings integrated into the waveguide

G.D. Marshall *et al.*, Opt. Lett. **33**, 956 (2008)

Femtosecond laser microfabrication for optofluidics applications

March 1, 2001 / Vol. 26, No. 5 / OPTICS LETTERS 277

Femtosecond laser-assisted three-dimensional microfabrication in silica

Andrius Marcinkevičius and Saulius Juodkazis

Satellite Venture Business Laboratory of Photonic Nano-Materials, University of Tokushima, 2-1 Minamijyosanjima, Tokushima 770-8506, Japan

Mitsuru Watanabe, Masafumi Miwa, Shigeki Matsuo, and Hiroaki Misawa

Department of Ecosystem Engineering, University of Tokushima, 2-1 Minamijyosanjima, Tokushima 770-8506, Japan

Junji Nishii

Optical Materials Division, Osaka National Research Institute, 1-8-31 Midorigaoka, Iketa, Osaka 563-8577, Japan

- Novel technique for the fabrication of directly buried microchannels in three dimensions

Femtosecond Laser Microchannel fabrication

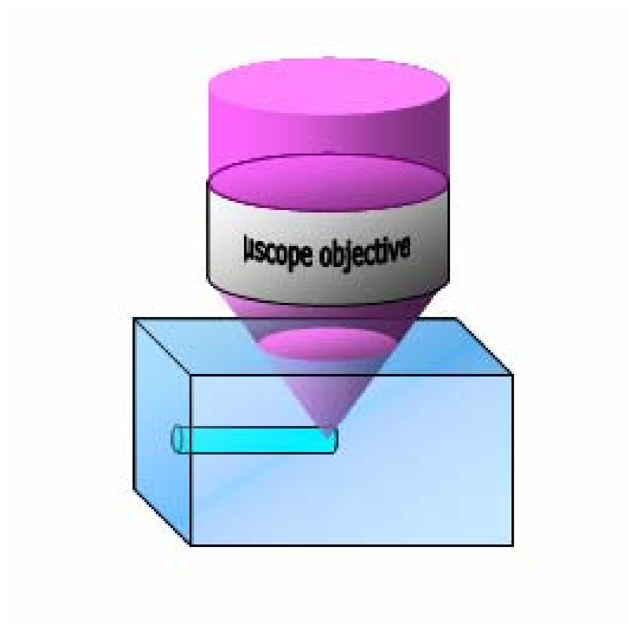

Femtosecond irradiation

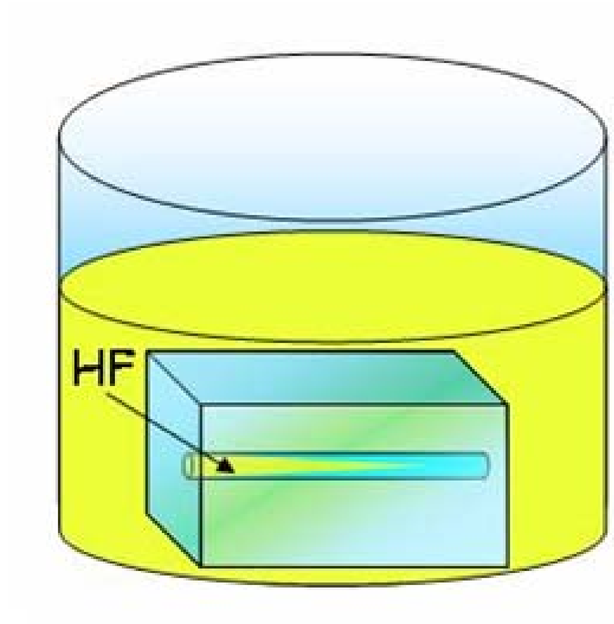

Chemical etching in HF

- High intensity femtosecond laser irradiation
- Selective etching in HF solution
- Fabrication of directly buried microchannels in three dimensions

Microchannel fabrication: underlying physical mechanism

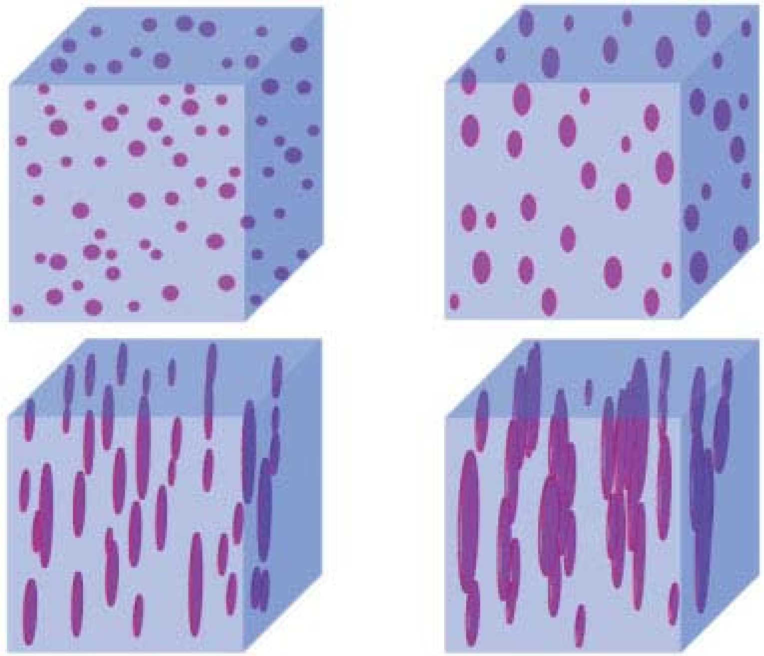

- Nonlinear ionization creates randomly localized plasma nanodroplets
- The droplets grow and flatten under the electric field
- They merge to form regular arrays of nanoplanes

R. Taylor et al., Laser Photonics Reviews **2**, 26 (2008)

Experimental evidence for the nanogratings

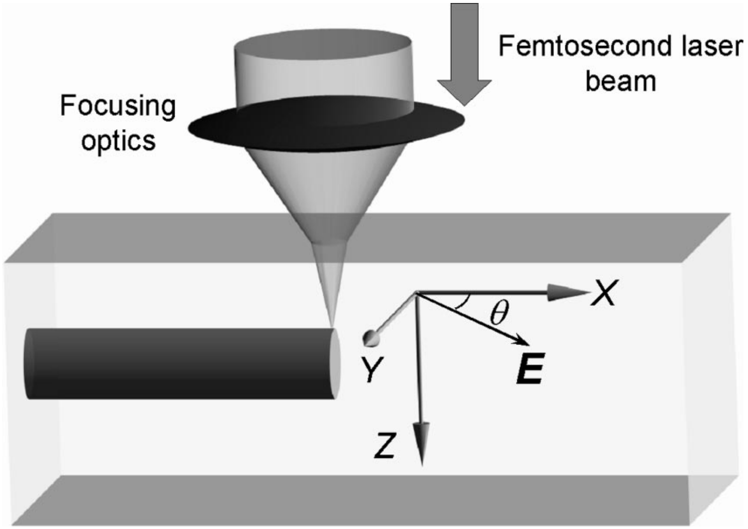

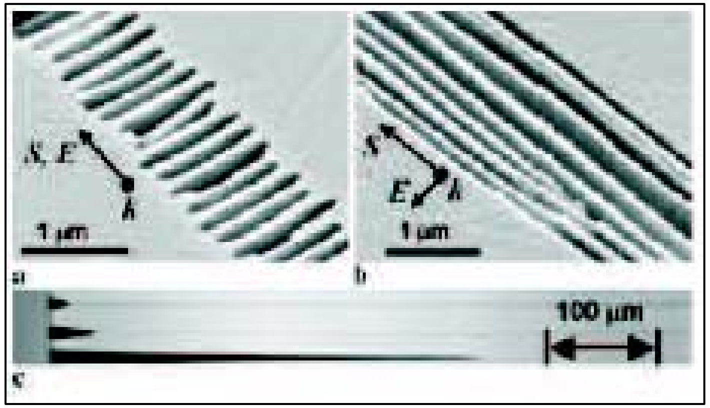

C. Hnatovsky *et al.*, Opt. Lett. **30**, 1867 (2005).

- Femtosecond laser irradiation followed by etching
- Grating planes are perpendicular to the direction of electric field
- Much higher etching rate when gratings are aligned along the writing direction

Microfluidic channels: characteristics

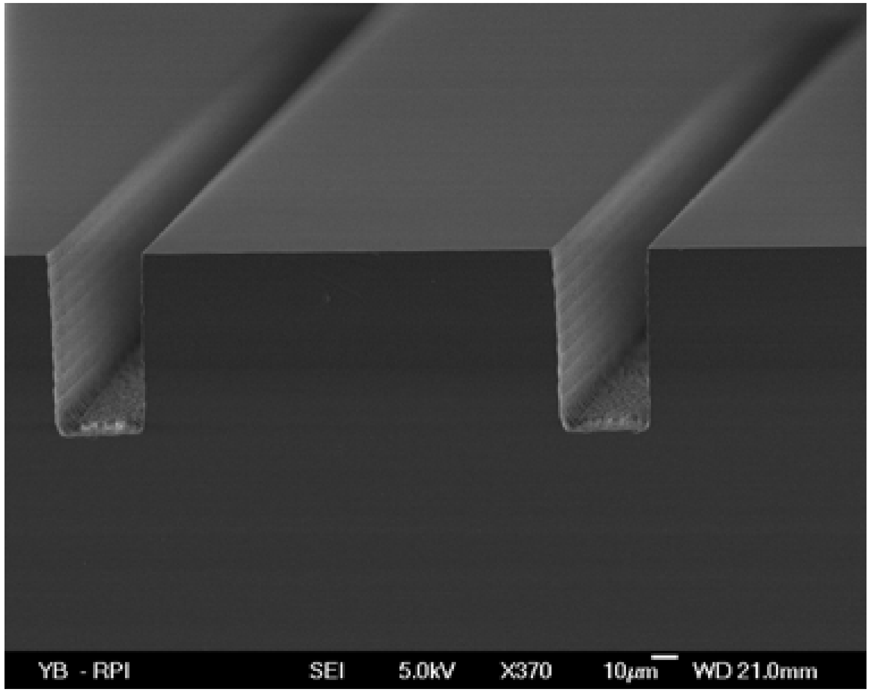

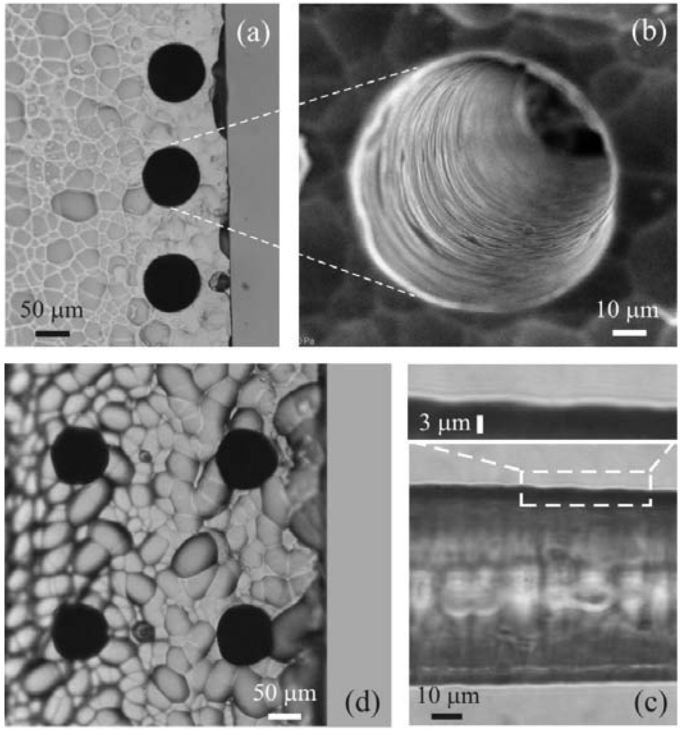

- High aspect ratio surface channels
- 3D directly buried channels

V. Maselli *et al.*, Appl. Phys Lett. **88**, 191107 (2006).

Y. Bellouard *et al.*, Opt. Express **12**, 2120 (2004).

Shape control of the microchannels

- Conical shape is intrinsic in the etching process of uniform structures

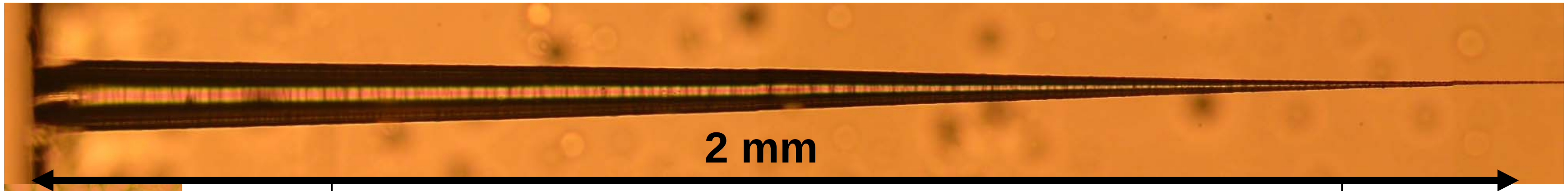

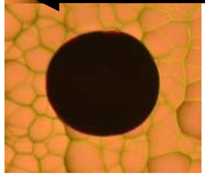

Wobbling the writing laser provides a perfectly uniform cylindrical channel

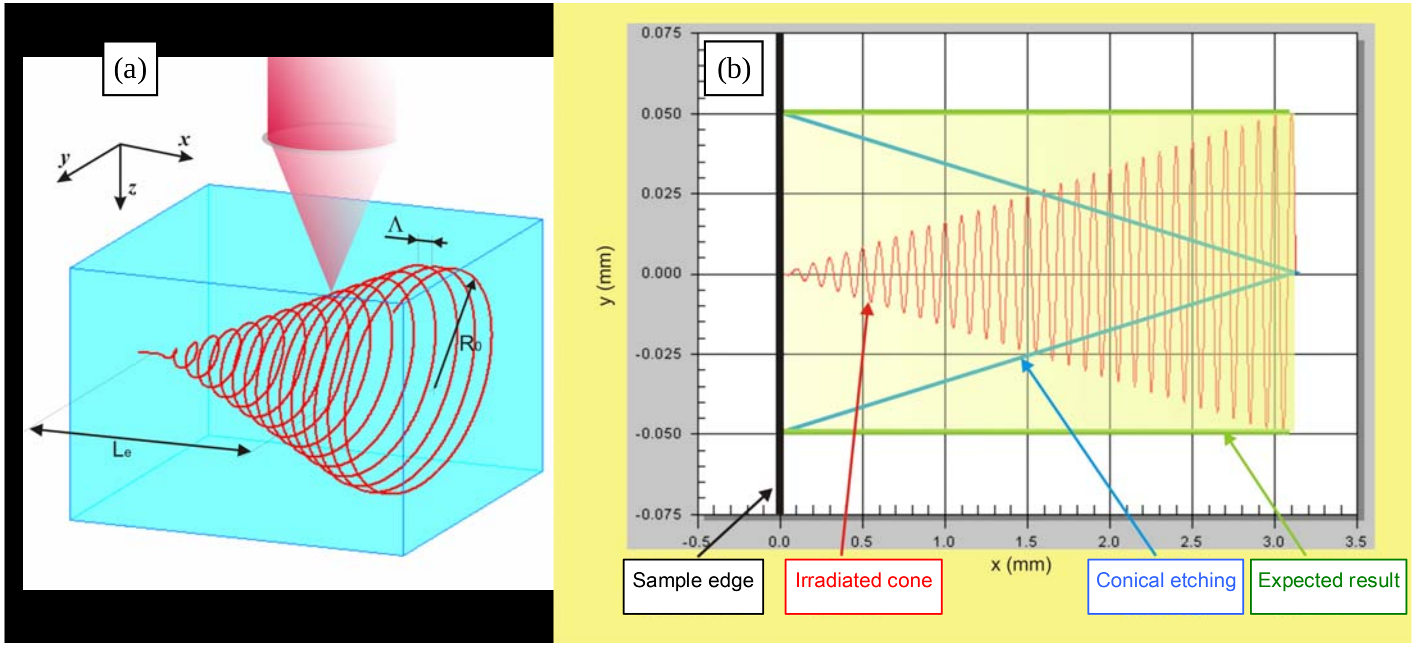

K. Vishnubhatla *et al.*, Opt. Express. **17**, 8685 (2009).

Shape control of the microchannels

- Conical shape is intrinsic in the etching process of uniform structures

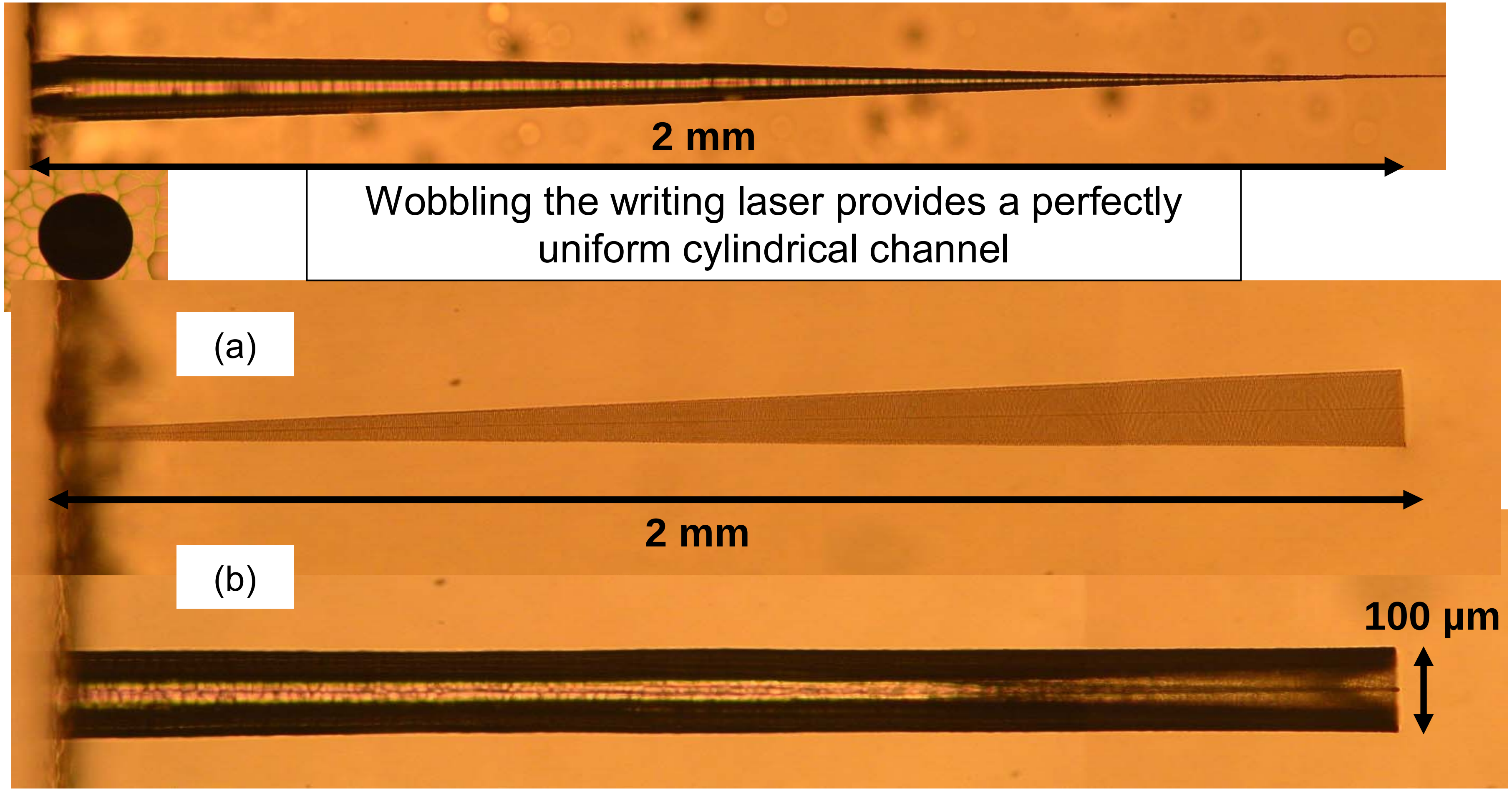

K. Vishnubhatla *et al.*, Opt. Express. **17**, 8685 (2009).

NATURE|Vol 442|27 July 2006|doi:10.1038/nature05060 INSIGHT REVIEW

Developing optofluidic technology through the fusion of microfluidics and optics

Demetri Psaltis[1], Stephen R. Quake[2] & Changhuei Yang[1]

We describe devices in which optics and fluidics are used synergistically to synthesize novel functionalities. Fluidic replacement or modification leads to reconfigurable optical systems, whereas the implementation of optics through the microfluidic toolkit gives highly compact and integrated devices. We categorize optofluidics according to three broad categories of interactions: fluid–solid interfaces, purely fluidic interfaces and colloidal suspensions. We describe examples of optofluidic devices in each category.

Optofluidics

- Liquids may improve or extend the functionalities of integrated optical devices

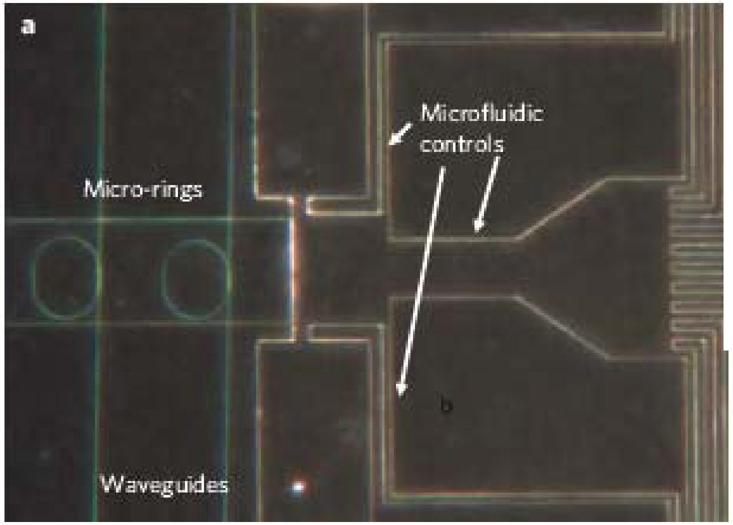

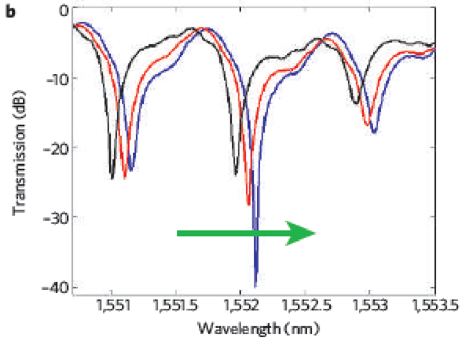

U. Levy et al, APL 88,111107 (2006)

- Integrated optics may enhance the sensing capabilities in fluidic devices

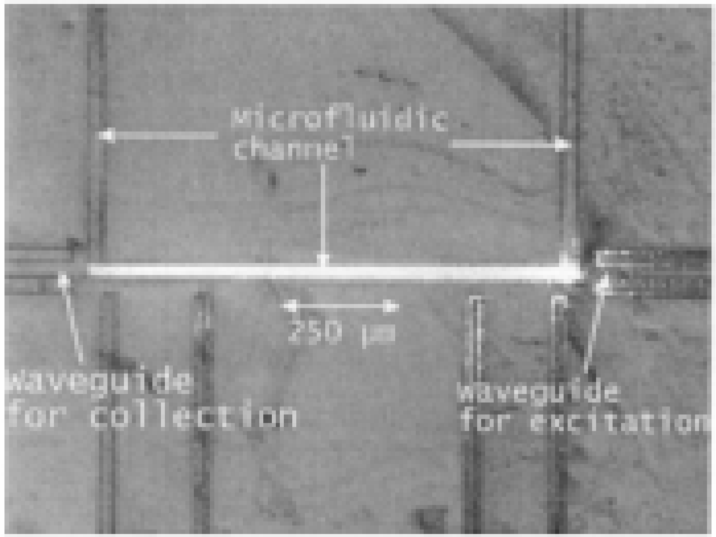

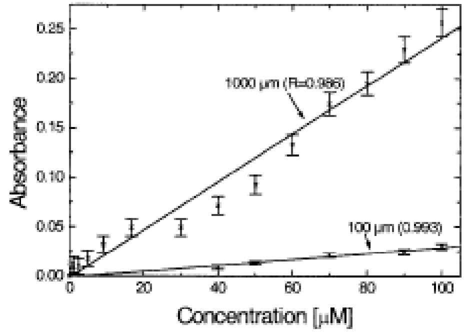

K.B. Mogensen et al, AO 42, 4072 (2003)

Femtosecond Micromachining for Optofluidics

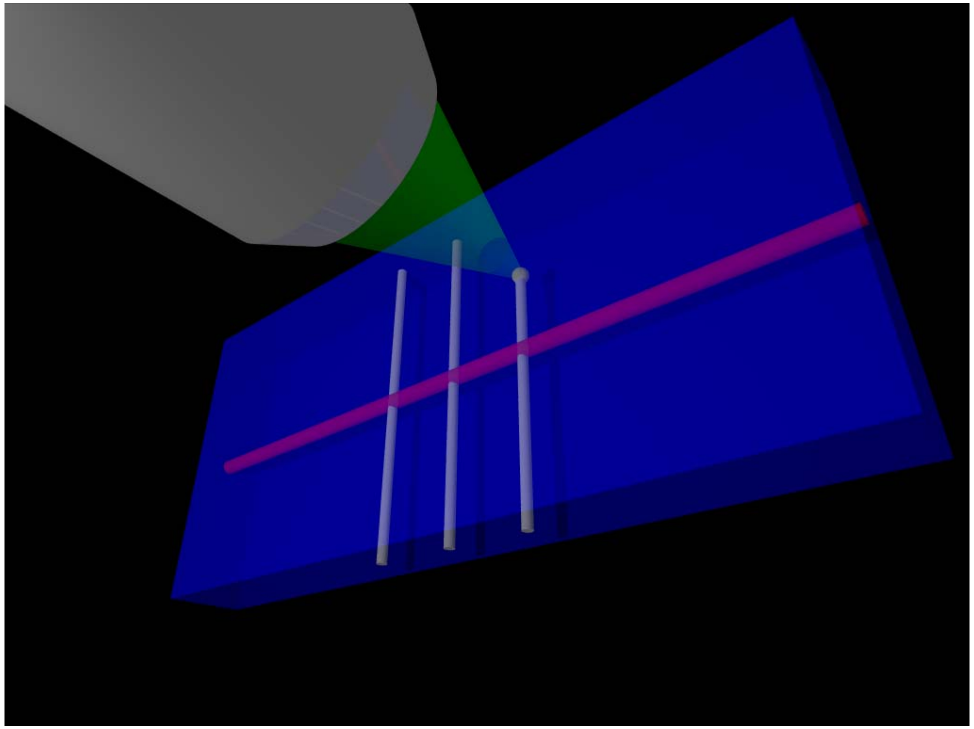

- Direct femtosecond laser fabrication of integrated waveguides and microchannels
- Use laser as post-processing tool adding new functionalities to microfluidic devices

Integration of femtosecond written waveguides and microchannels

- Single side: 1.8mm, ∅90μm
- Double side: 3mm, ∅100-50μm or 2.2mm, ∅110-90μm

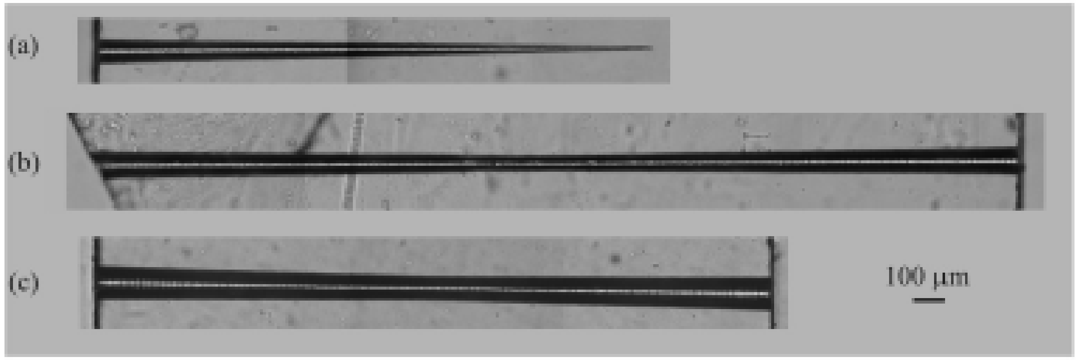

- Waveguides provide selective excitation of a Rhodamine solution in the channel

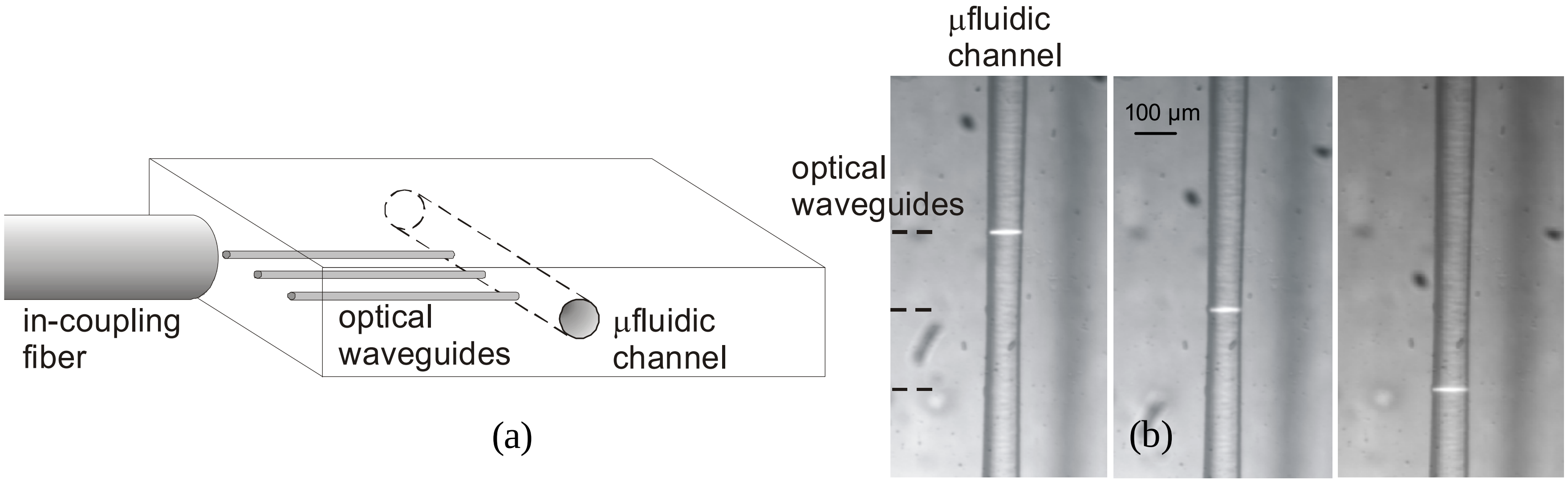

R. Osellame *et al.*, Appl. Phys. Lett. **90**, 231118 (2007).

Femtosecond laser written optofluidic cell detector

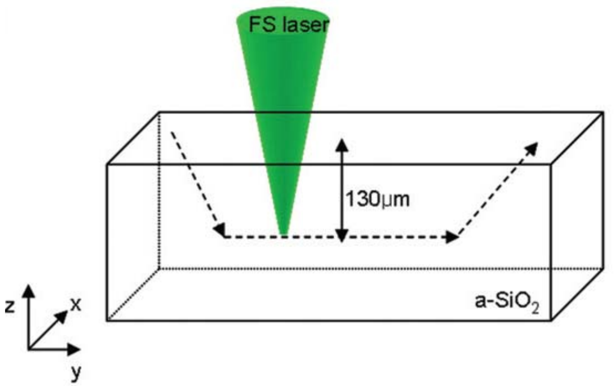

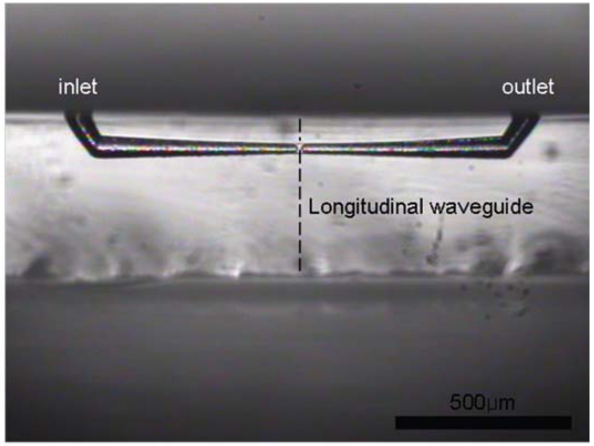

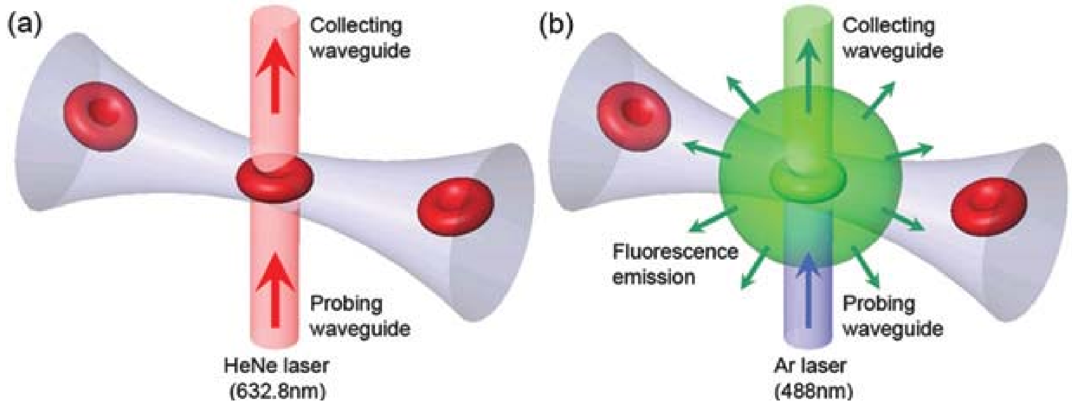

M. Kim *et al.*, Lab on Chip **9**, 311 (2009)

Lab-on-a-Chip

A **network of microfluidic channels** allows to perform **chemical processes** or **bio-analysis** with very small amounts of fluids

- Extreme miniaturization:
  - Rapid and automated processes
  - Limited reagents consumption
  - Capillarity and surface interactions
- Multifunction integration
  - microfluidics + analytical techniques
  - replicate a real chemi/bio-lab on chip

Our approach

On-chip optical sensing by means of femtosecond laser written 3D photonic devices

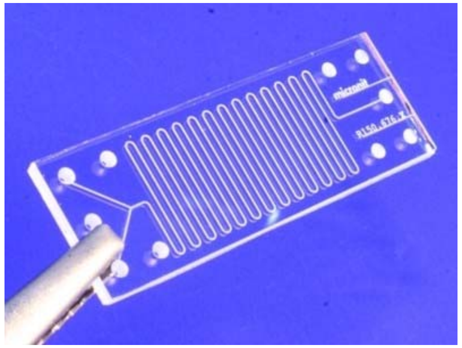

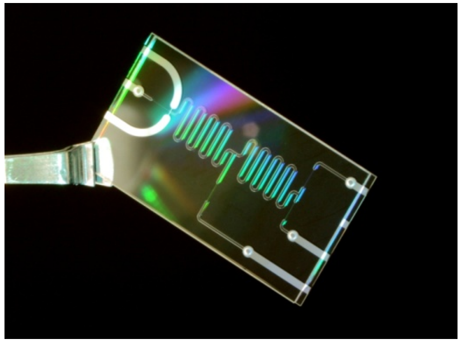

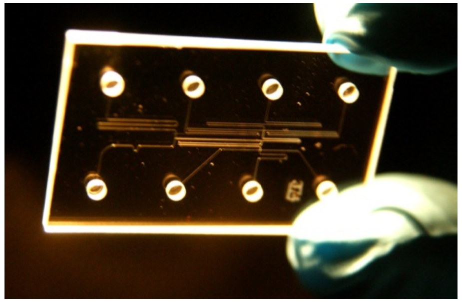

Capillary electrophoresis in *Lab on a Chip*

1) Injection

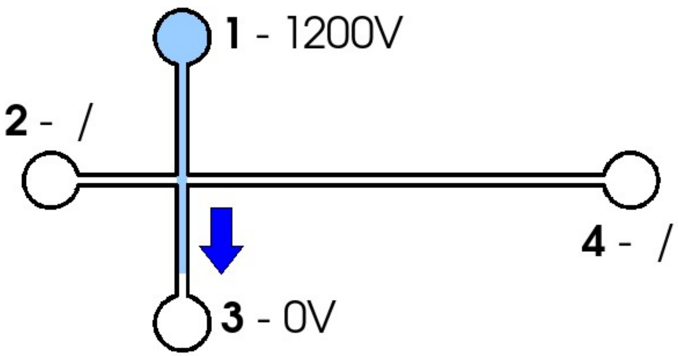

3) Detection

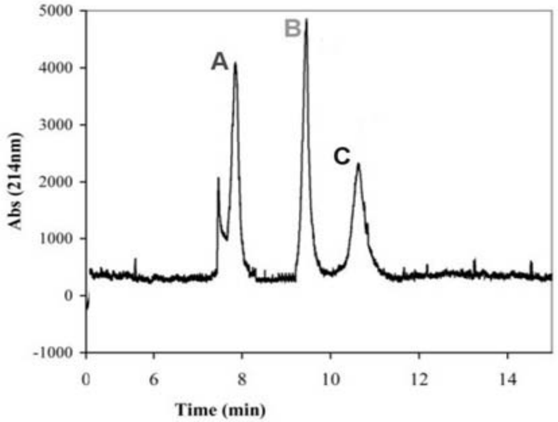

The **flow of molecules** is driven by **voltages** applied to the reservoirs

2) Separation

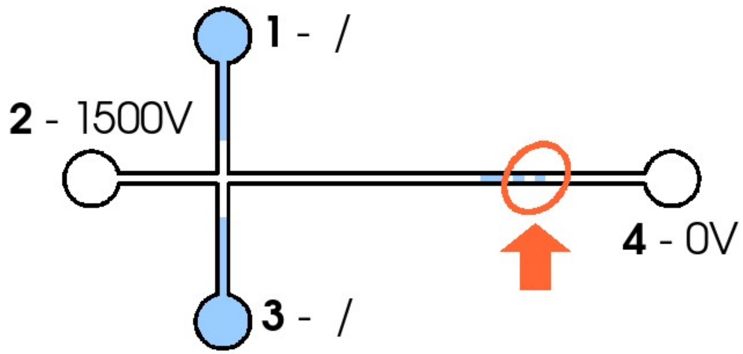

Molecules will separate in the channel according to the **different mobility**

They are **identified** on the basis of the **arrival time** at the detection point

Microchip capillary electrophoresis

Application: separation of DNA fragments to perform bioassays for the detection of a variety of diseases.

Exogenous DNA detection: viruses and bacteria.

Endogenous DNA mutation detection: cancer, hereditary genetic diseases

Detection techniques

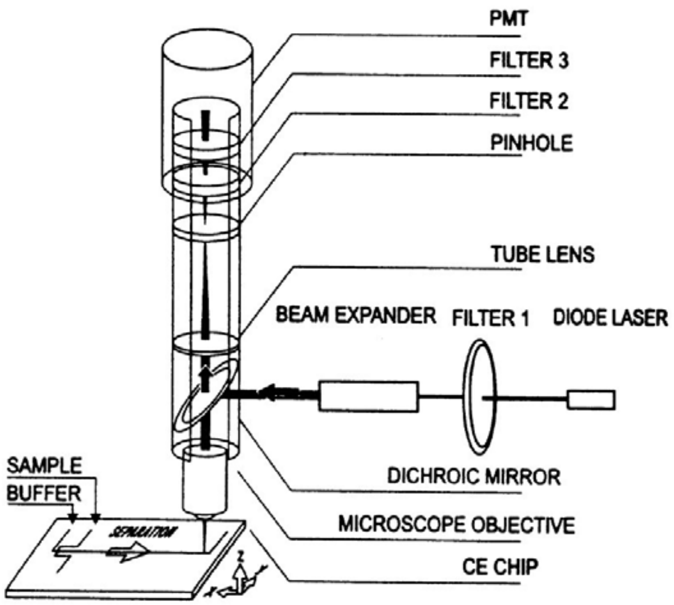

Confocal microscope for *off-chip* detection

Optical detection

- Fluorescence
- Absorbance
- Refractive index

***Off-chip* approach**

External bulky equipment that needs precise alignment

⇓

Lab-on-chip miniaturization is frustrated

***On-chip* approach**

Monolithic integration of photonic devices with one-time alignment

Increased compactess and portability but increased fabrication complexity

Femtosecond laser post-processing of lab-on-chips

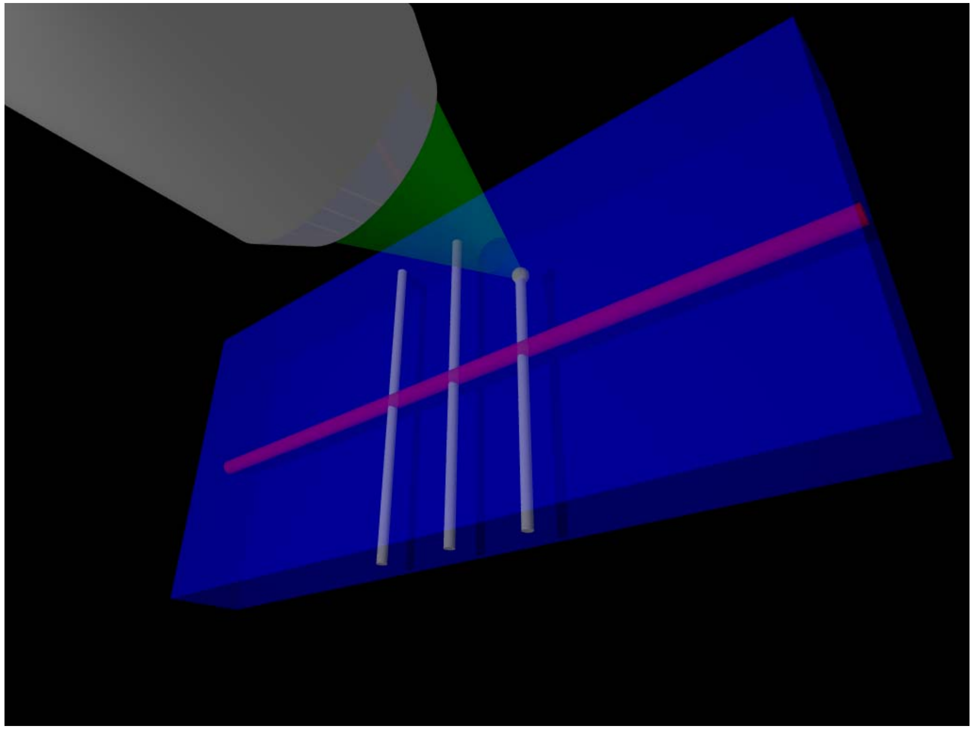

- Post-processing on an already made Lab-on-a-chip.
- Fabrication of three-dimensional devices.
- High versatility and limited equipment costs.

On-chip waveguide integration

- **Commercial** microfluidic chip for capillary electrophoresis (by LioniX bV)

µchannel 1-3 for injection
µchannel 2-4 for separation

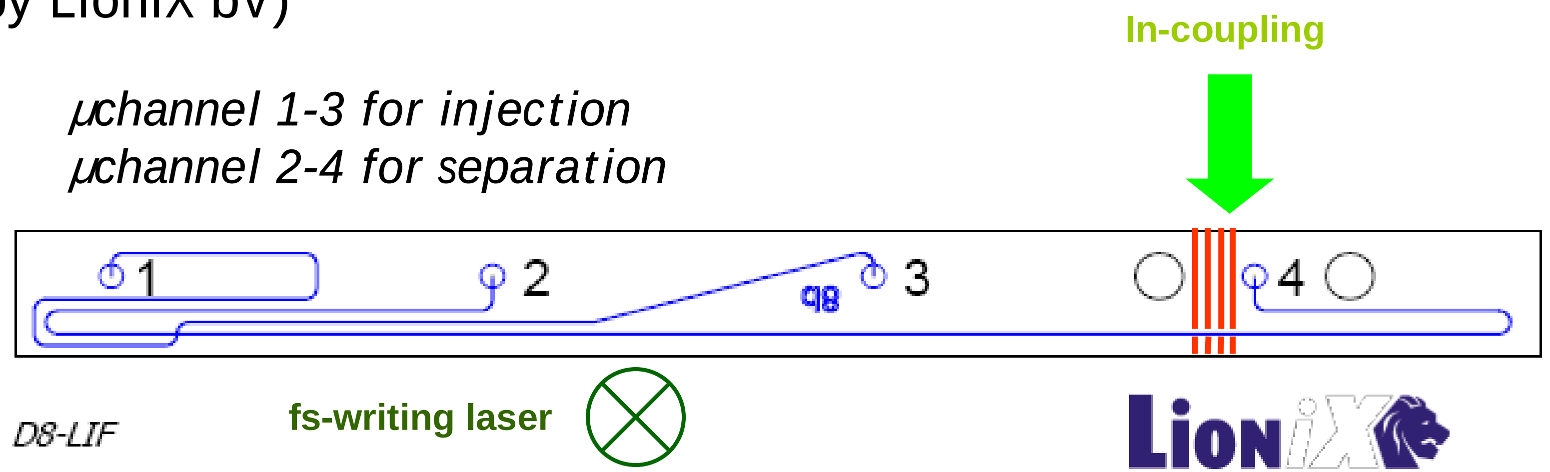

- Microchannel cross-section

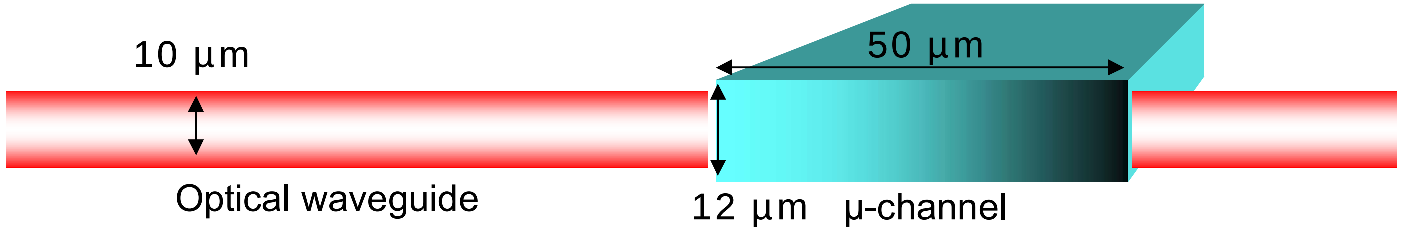

On-chip waveguide integration

➢ Inscribed optical waveguide allows **selective excitation** in the channel

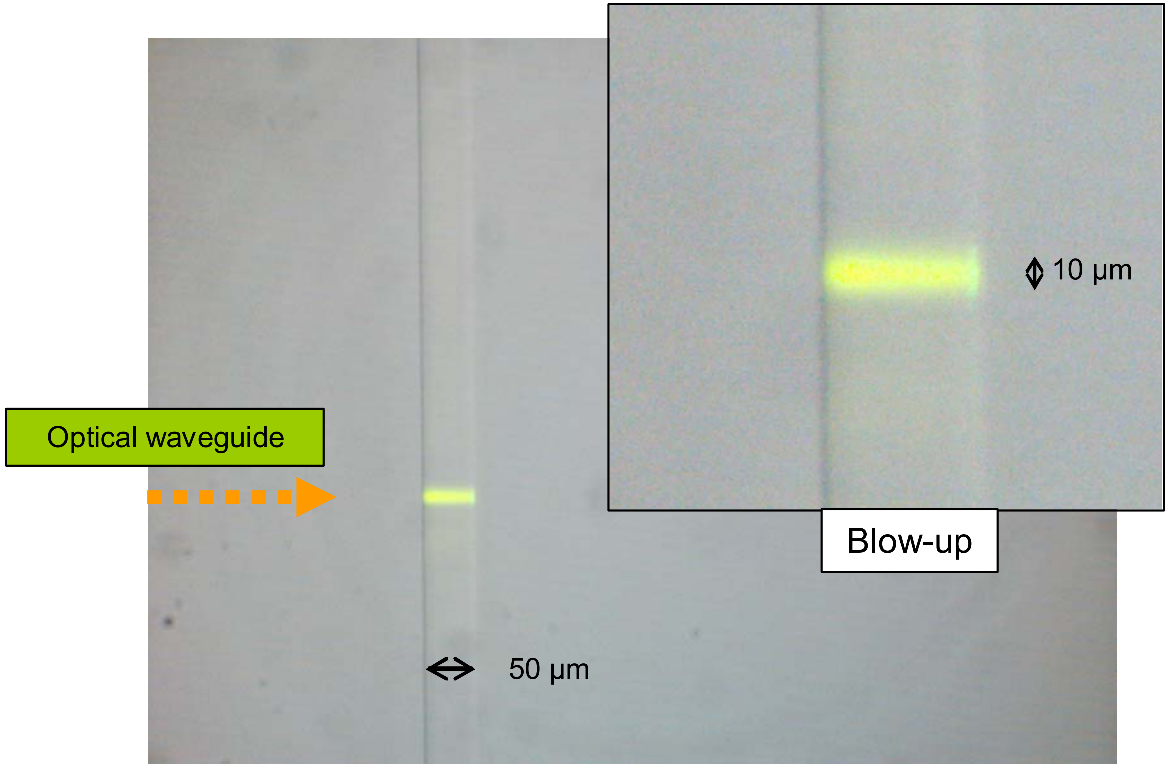

Laser at 532 nm coupled into the waveguide

Microchannel filled with rhodamine 6G
Microscope image through a cut-off filter at 570 nm

On-chip waveguide integration

- Pigtailed excitation and collection fibers provide a very **compact** and **portable** unit

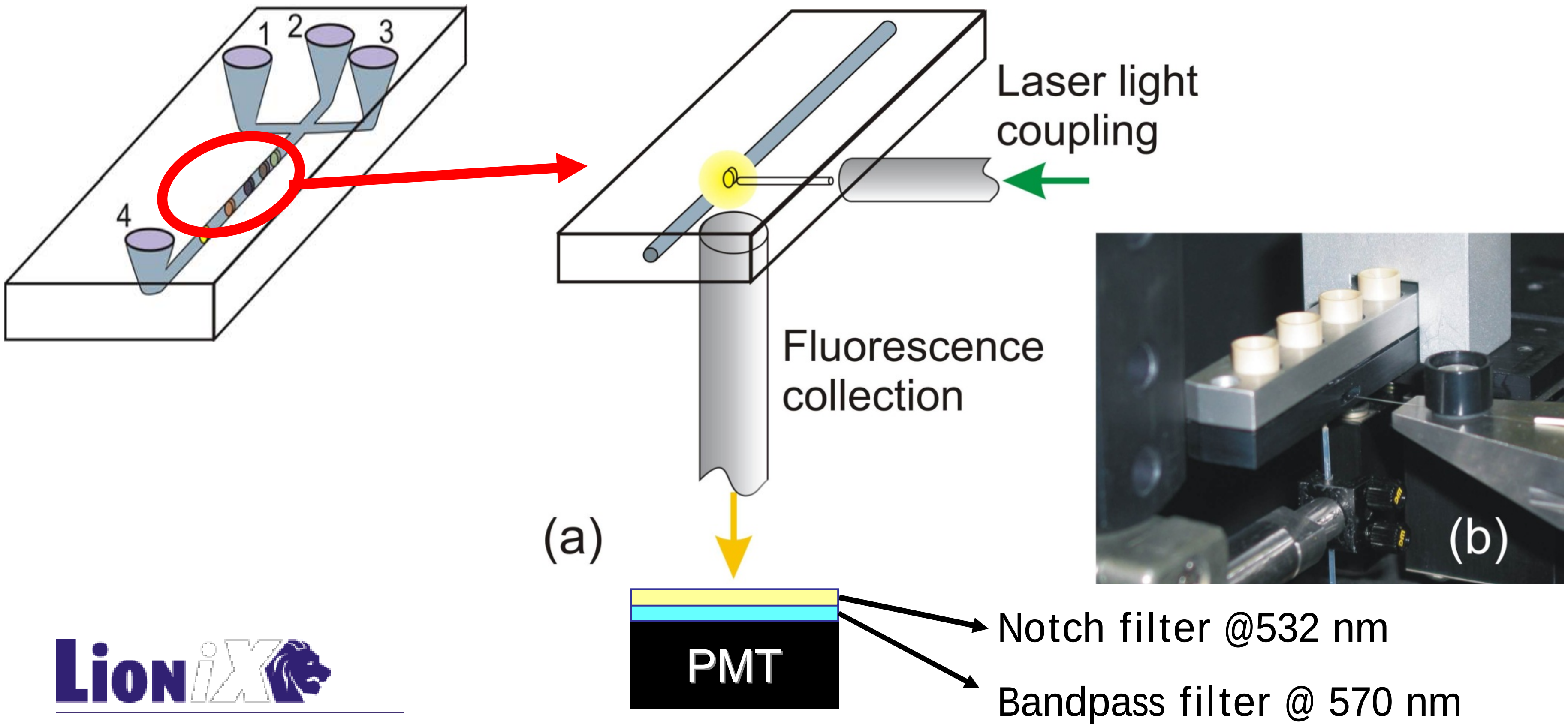

LioniX

On-chip Laser Induced Fluorescence detection

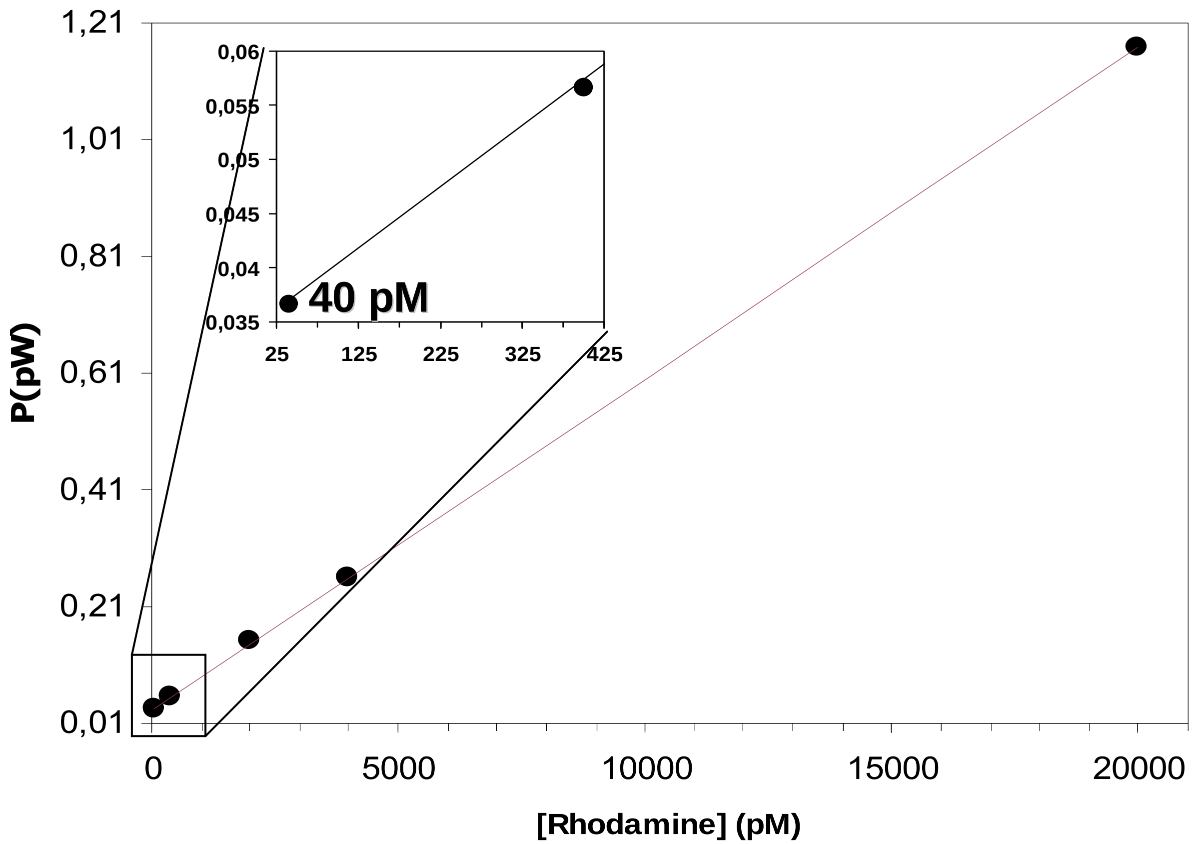

- Rhodamine 6G
- 100 µW of 532 nm excitation
- Detection filter 570±5 nm

➢ **Limit of detection ~10 pM**, among the best results for integrated detection

R. Martinez Vazquez *et al.*, Lab Chip **9**, 91 (2009)

Dynamic detection of separated molecules

- CCD imaging of laser induced fluorescence by a fs-laser written waveguide
- Sample is a highly concentrated solution of two different dyes (Rhodamine 6G and Rhodamine B)

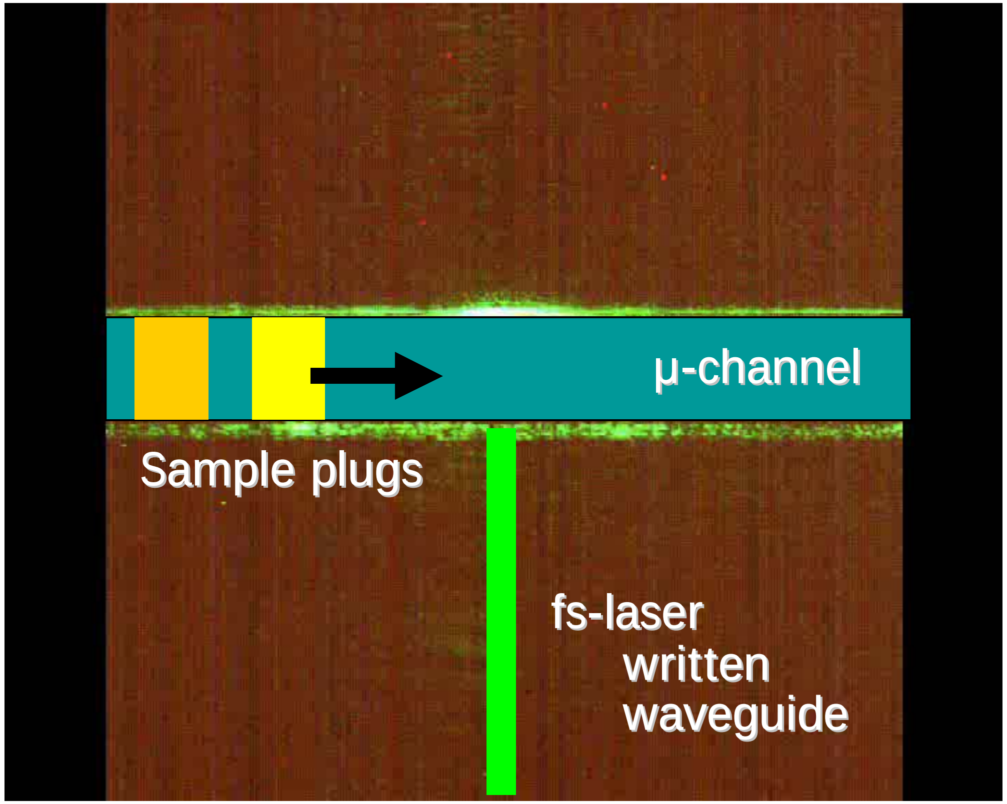

C. Dongre *et al.*, Opt. Lett. **33**, 2503-2505 (2008).

Dynamic Detection of labelled DNA fragments

- **Oligonucleotides** (23 mer) labelled with Cy3
- Polymer coating of the inner walls of the channels to inhibit electroosmotic flow
- Electrophoretic flow under electric fields

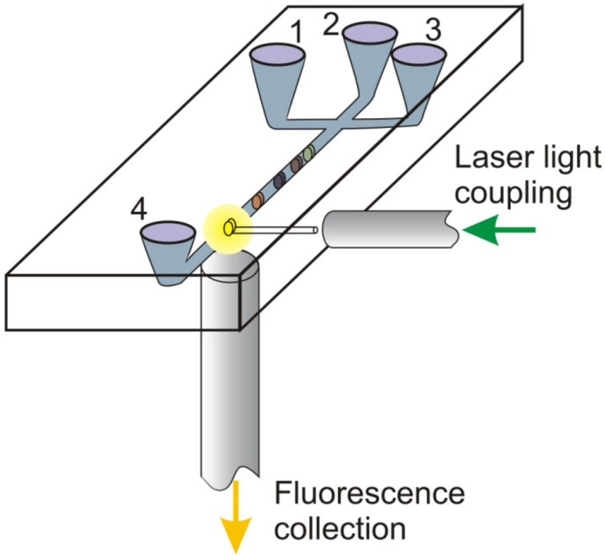

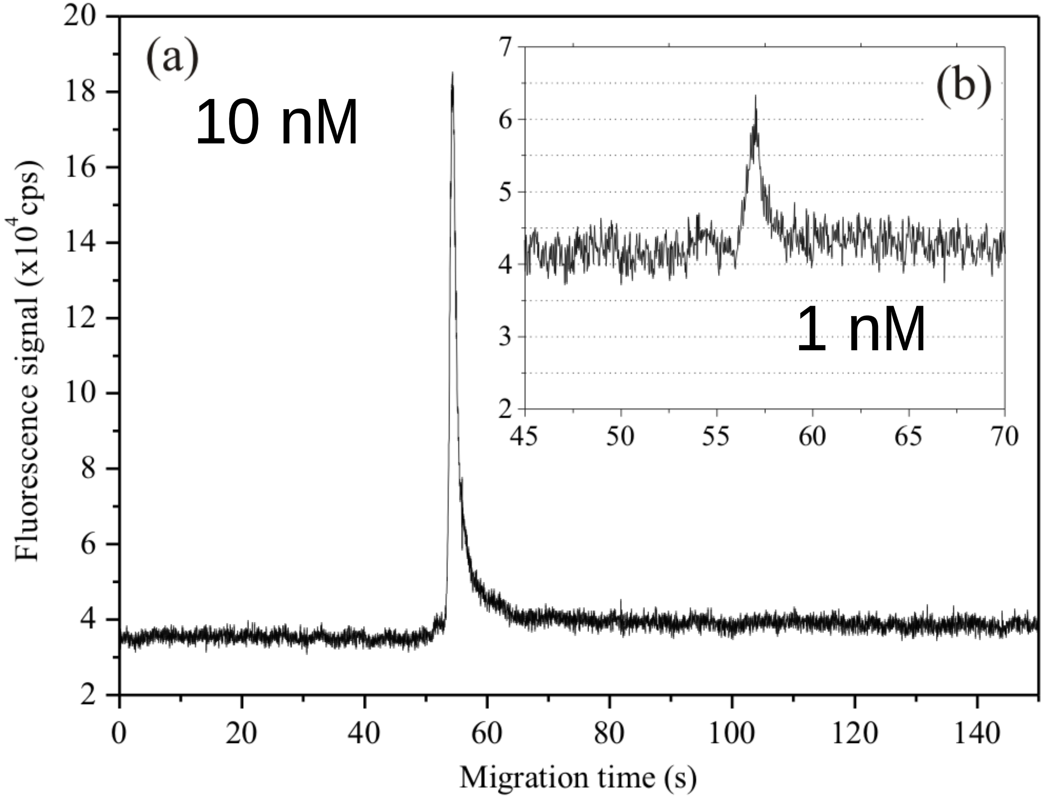

1 nM dynamic LOD

SNR ~ 10

Refractive index sensing

Monitoring chemical reactions in microreactors through interferometry in the **Mach-Zehnder** configuration

- Need for **spatial resolution** ⇒

  interferometer **orthogonal** to the separation channel

- Channel width of only L = 50 μm ⇒

  evanescent field sensing too weak ⇒

  one arm of the interferometer is **crossing the channel**

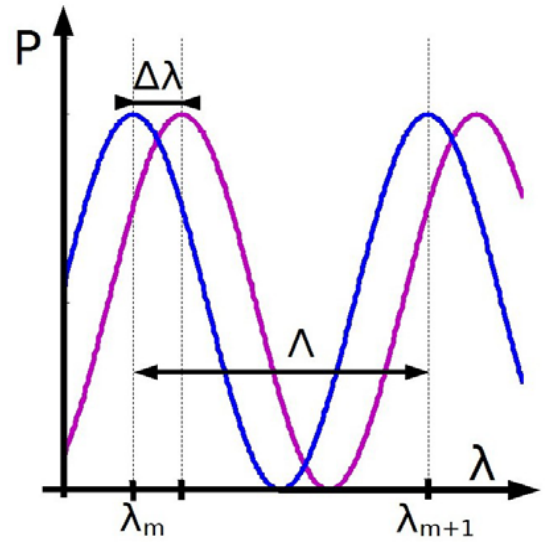

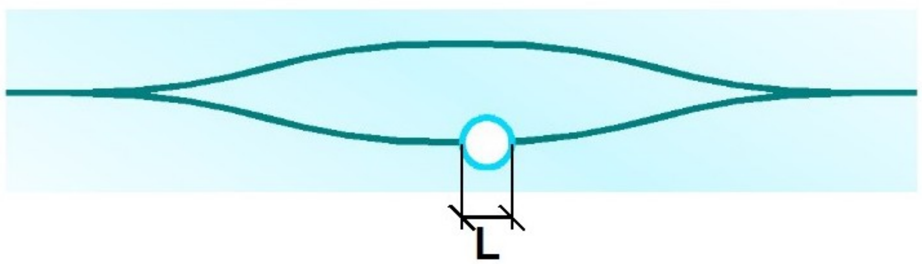

Fringe shift

The phase shift acquired in the channel induces a fringe shift

Mach-Zender integration

Tilting of 7°

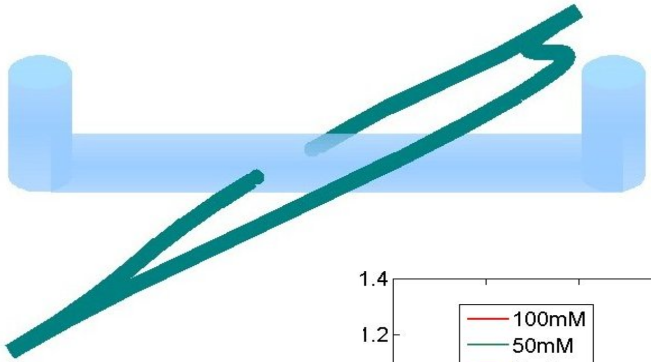

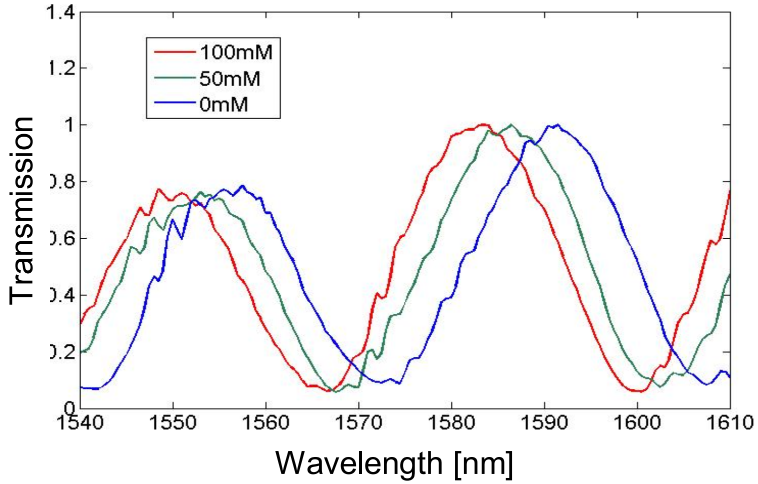

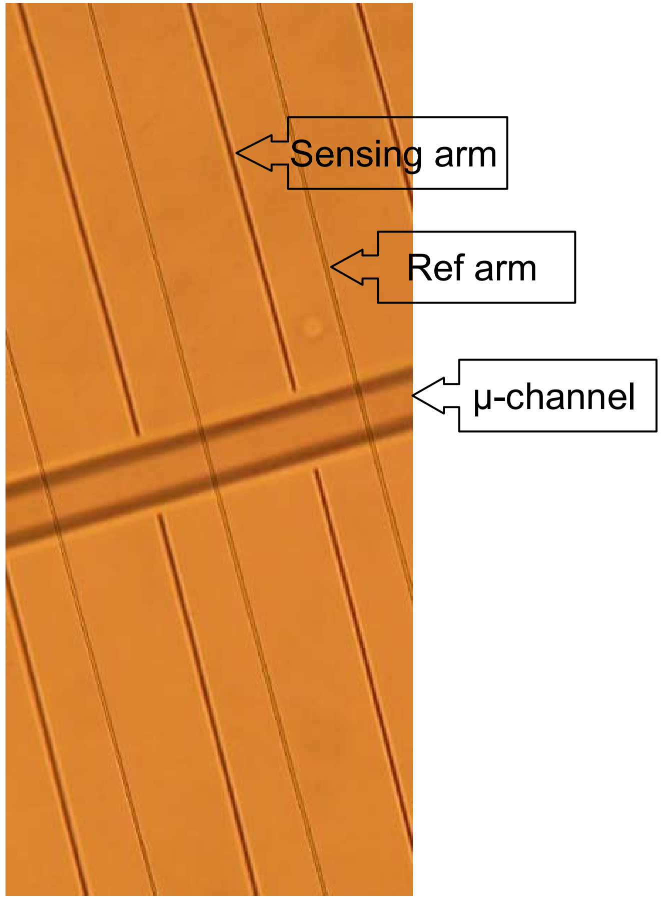

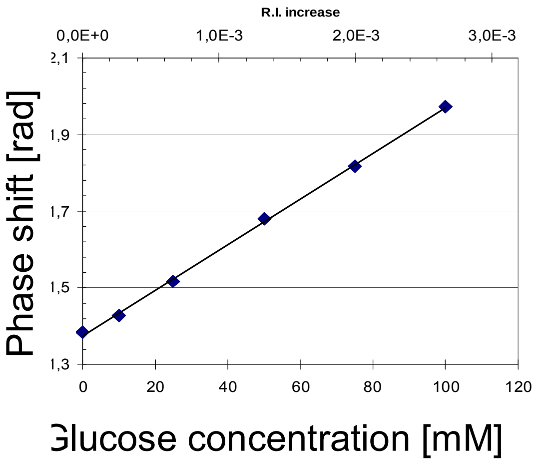

10 mM of glucose provides a very clear fringe shift

$\Rightarrow$ Sensitivity of at least $\Delta n=1\times10^{-4}$

Microchannel shaping applications

- Channel with top access holes (U-shape)

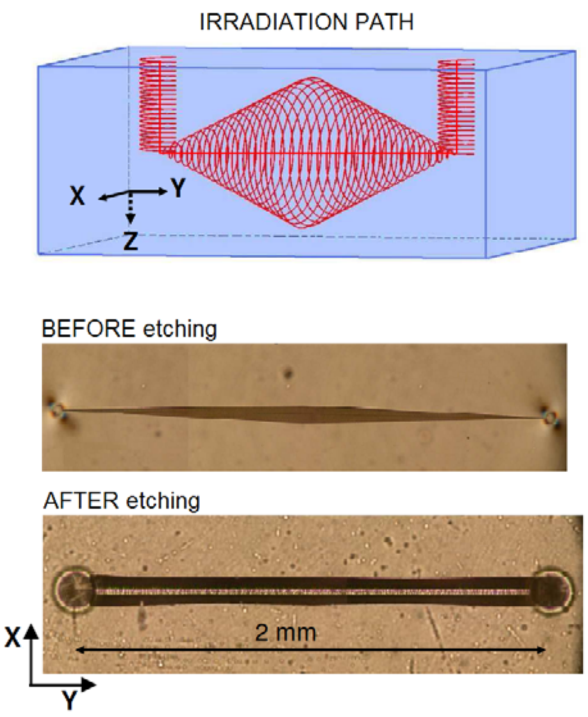

- Fannel-shape channel (shape control along the channel axis)

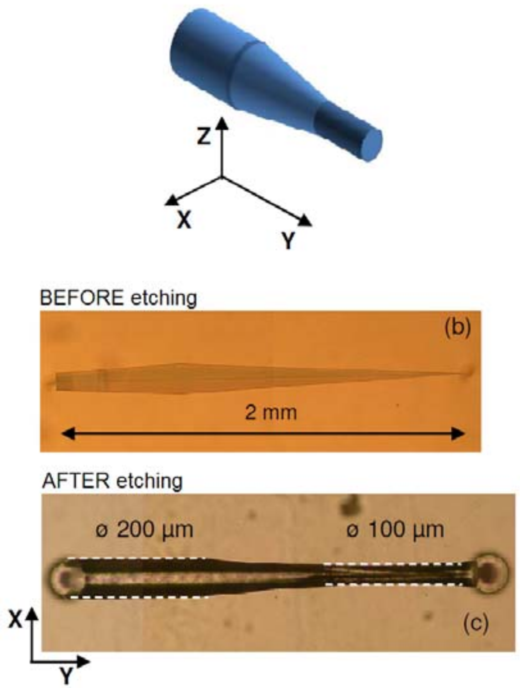

- O-groove for fiber coupling

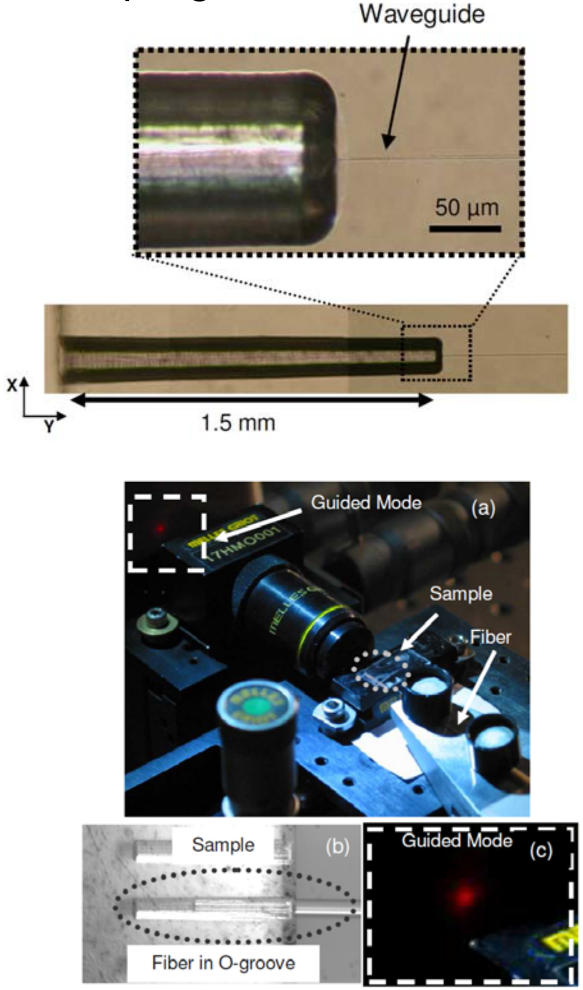

Optical stretcher

Optical dual-beam trap for single cell (*1μm wavelength*):
- non-focusing counter-propagating beams can trap single cells
- increasing the optical power the trapped cell is stretched along the beam axis

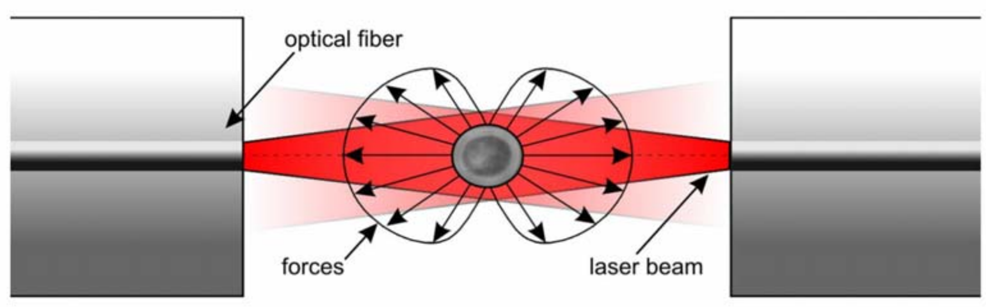

standard configuration: cell suspension in between 2 counter-propagating *fibers*

• misalignement between discrete optical and fluidic components

• system suffers for vibrations and fluctuations

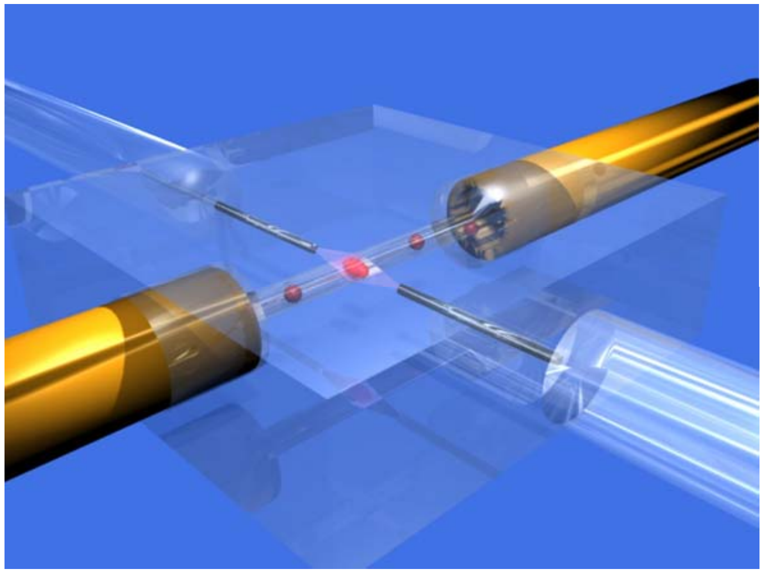

monolithic configuration: optical waveguides crossing the microfluidic channel with the flowing cell suspension in a *glass chip*

• no alignement + vibration problems

• higher system portability

• possibility of adding other waveguides for further optical funcionalities

Optical stretcher: fabrication

- Microchannel fabrication with larger access holes for capillary connection

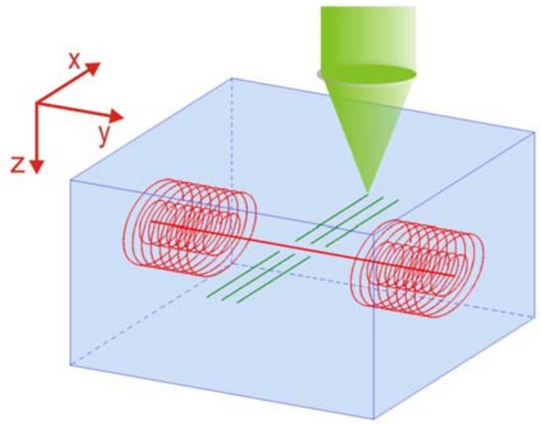

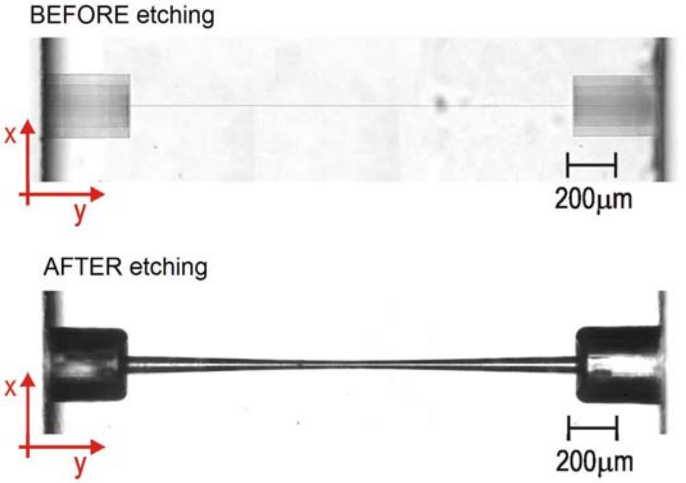

- "self-aligned" optical waveguides at different distance and depth with respect to the channel

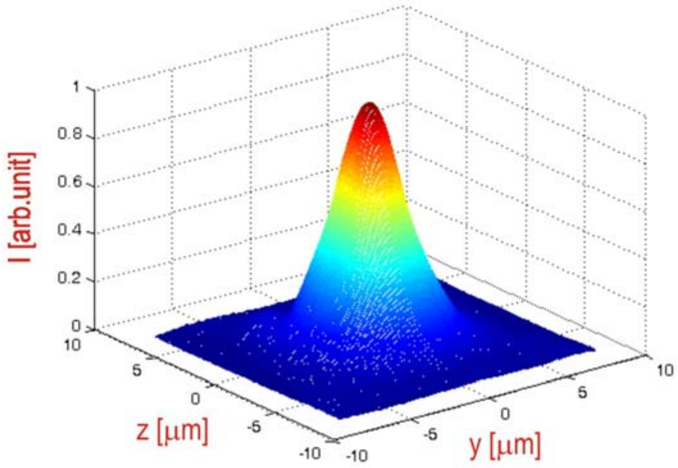

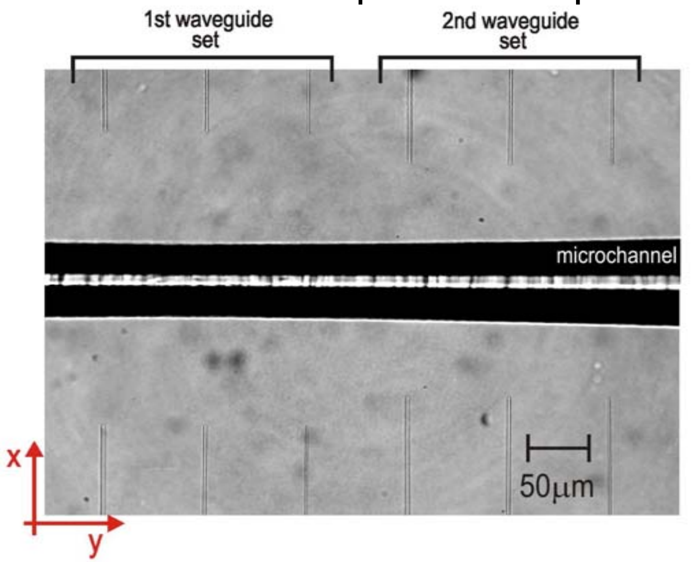

Optical stretcher: experimental results

Test the system on
red blood cells (RBCs)

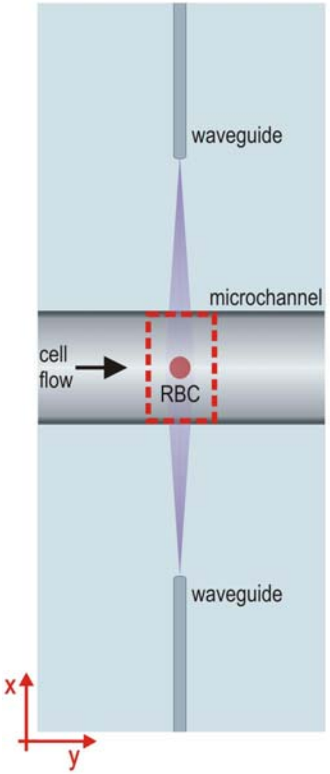

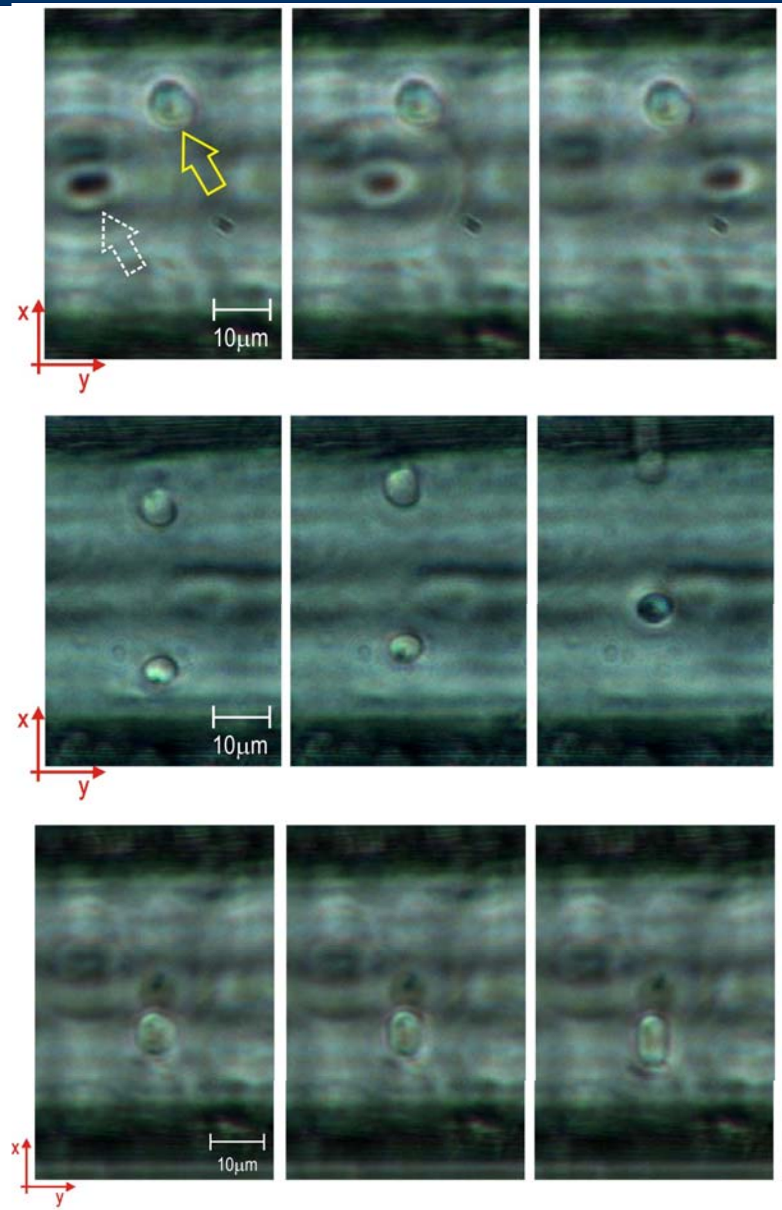

TRAPPING

balancing optical power at the two waveguides (P_{opt}≈20mW)

MOVING

unbalancing the power at the two waveguides

STRETCHING

simoultaneously increasing the power at the two waveguides (P_{opt}≈300mW)

Conclusions

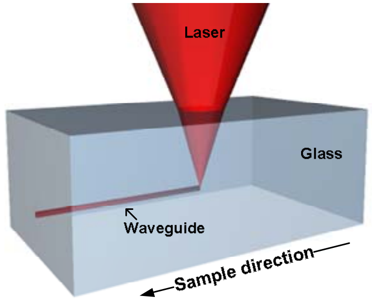

- Femtosecond writing is a simple and powerful technique for the direct fabrication of high quality optical waveguides

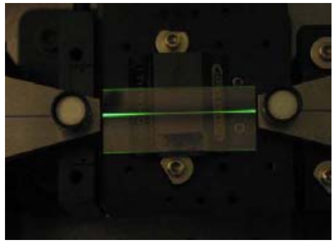

- A variety of passive and active devices, both 2D and 3D, can be manufactured in various glass substrates

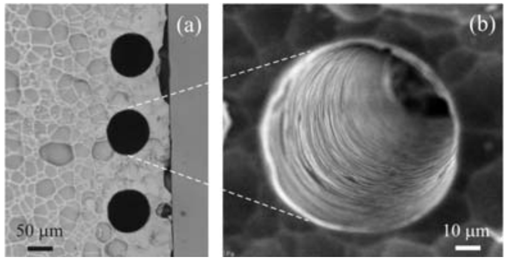

- Femtosecond laser irradiation + etching provides directly buried 3D microchannels

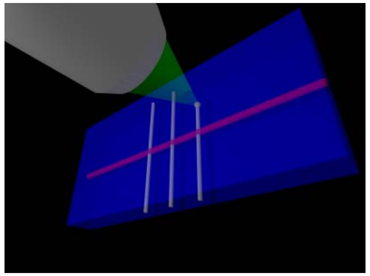

- Waveguides and channels can be integrated in different geometries to implement optofluidic functionalities

Financial support

DACO
5° FP EU CRAFT-project

HIBISCUS

6th FP EU STREP-project

www.fisi.polimi.it/hibiscus

microFLUID

7th FP EU STREP-project

www.fisi.polimi.it/microfluid

Acknowledgements

Politecnico di Milano – Department of Physics

Giulio Cerullo (femtosecond laser group)

Paolo Laporta, Giuseppe Della Valle, Stefano Taccheo (solid-state lasers)

Guglielmo Lanzani (organic materials)

Marco Marangoni (integrated optics)

IFN-CNR

Roberto Osellame (integrated optics and optofluidics)

Rebeca Martinez Vazquez (optofluidics)

Tersilla Virgili (organic materials)

Post-Doc and PhD

Krishna C. Vishnubhatla

Shane Eaton

Nicola Bellini, Nicola Chiodo, Andrea Crespi, Valeria Maselli

(Acknowledgments to N. Bellini, G. Cerullo, R. Osellame, K.C. Vishnubhatla for providing slides material)

Photovoltaics (Si-based): state of the art

Photovoltaic (PV) industry faces several challenges to achieve a competitive cost per kilowatt-hour for electricity over the life of the system :

- Cost-reduction of the solar cells or modules
- Enhancement of module efficiency

Thin-film technologies result in the lowest price-per-watt, but crystalline (wafer-based) solar cells exhibit the highest efficiency. Commercially available monocrystalline-silicon cells currently achieve 12% to 19% efficiency (far from the theoretical goal of 35%). Competing technologies: amorphous thin-film Si; cadmium telluride; copper indium germanium selenide; III/V triple junction cells; organic cells.

Losses are caused by light reflection, carrier recombination, ohmic losses, shadowing effects of the front contacts, and so forth.

New cell concepts are aimed at finding solutions to reduce these losses.

Backside contacts

Front contact patterning of a typical solar cell can shadow up to 10% of the photoactive area. To reduce such effect contacts can be taken through the backside of the solar cell: e.g. MWT (metal wrap through) approach

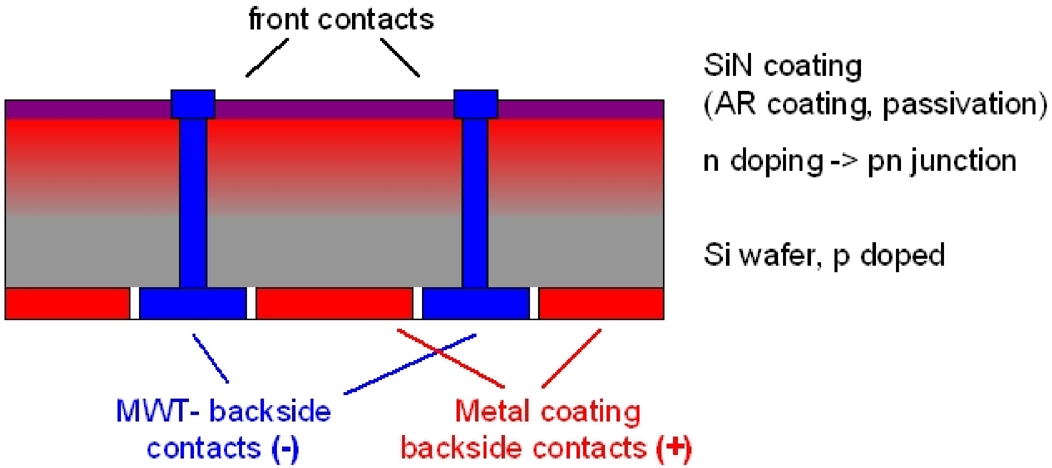

The MWT (metal wrap through) cell concept "wraps" front contacts to the cell backside. Complete backside wiring is a technological advantage and the wrapped front side contact can use a larger area. (Courtesy of Jenoptik)

For MWT 50 to 100 μm via holes must be drilled through 160-200 μm thick silicon wafers. Advantages: electrical connections to the cell and resistance (ohmic) losses are reduced because the dimensions of the contacts at the backside are no longer limited by shadowing effects. Around 100 holes per second to be drilled. Few 100-1500 ns laser pulses are sufficient for the drilling step, followed by post-processing (damage etching, silicon nitride coating, printing of electrical contacts. Efficiency increase in commercial cells 1%.

Are ns-laser pulses sufficient?

Nanosecond pulses may cause thermal effects during scribing that generate recombination centers in the bulk silicon. To reduce or prevent melting effects picosecond or femtosecond lasers can be used.

By using femtosecond laser pulses the shape of microscopic pyramidal structures is preserved even after scribing with the laser.

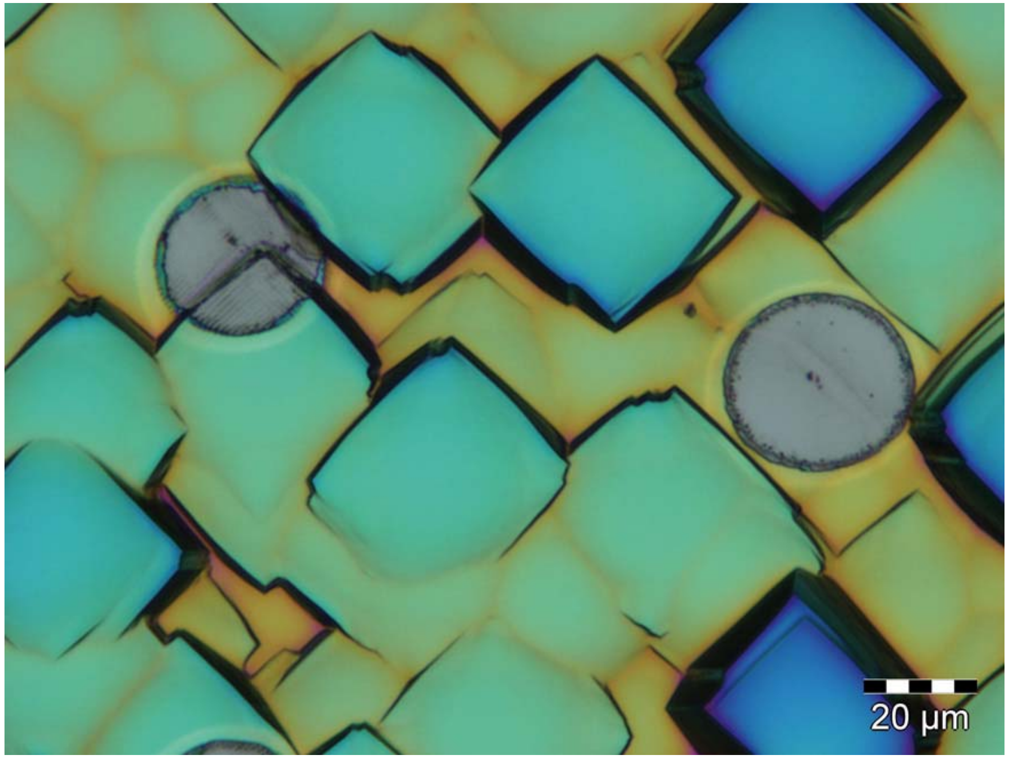

A micrograph shows c-Si surface structure after KOH etching. Single-shot femtosecond laser processing (round spots) preserves these structures without melting. (Courtesy of Jenoptik)

Selective doping

Within the frame of classical cell structure with frontside and backside contacts, laser diffusion or laser doping is a hot topic in crystalline solar-cell manufacturing to enhance cell efficiency.

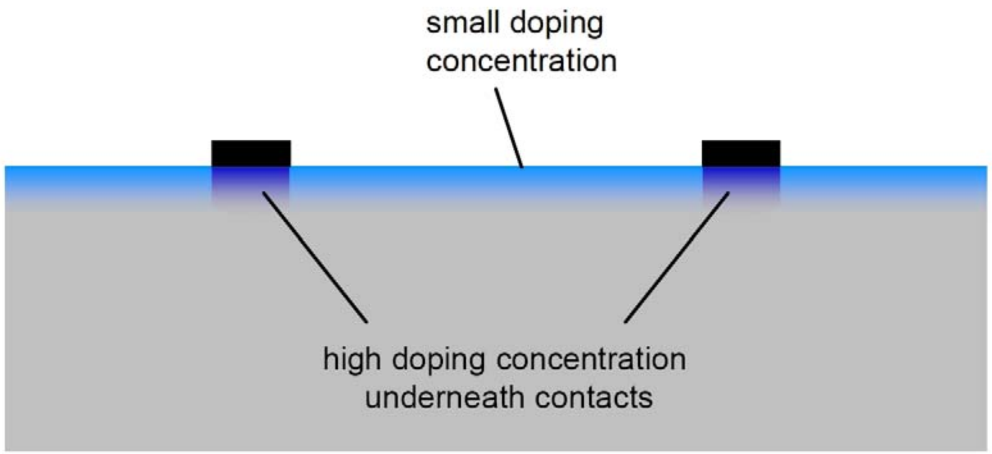

Selective emitter doping is a laser-based technique that can enhance PV cell efficiency by reduction of ohmic losses at the contacts. (Courtesy of Jenoptik)

Selective doping of the silicon allows reduction of the electrical resistance (ohmic losses) of the bulk silicon material underneath the contact fingers. Absolute cell efficiency increases by 0.3-0.5%. In this process a phosphorus coating diffuses from the surface into the bulk silicon at the locations where the silicon is melted by the laser (i.e. where the contact fingers are later located. The sheet resistance of laser-treated vs untreated area is strongly reduced, e.g. 120-150 ohm/sq to 20 ohm/sq. CW or ns-pulses high power lasers (hundreds of Watts) are required.

Texture is one of the critical surface parameters affecting solar-cell efficiency. A polished wafer of monocrystalline silicon (as in a bare semiconductor-grade silicon wafer) is about 40% reflective, depending on the wavelength of the incident radiation. A widely accepted technique to reduce this reflectivity is to texture (roughen) the surface so that reflected photons have a chance of being incident on another facet of the PV cell, creating another opportunity for PV interaction in the emitter layer. If the surface roughness is too great, however, then the mean free path (MFP) of the electron/hole pair may elongate to the point where the probability of them recombining reduces the overall efficiency.

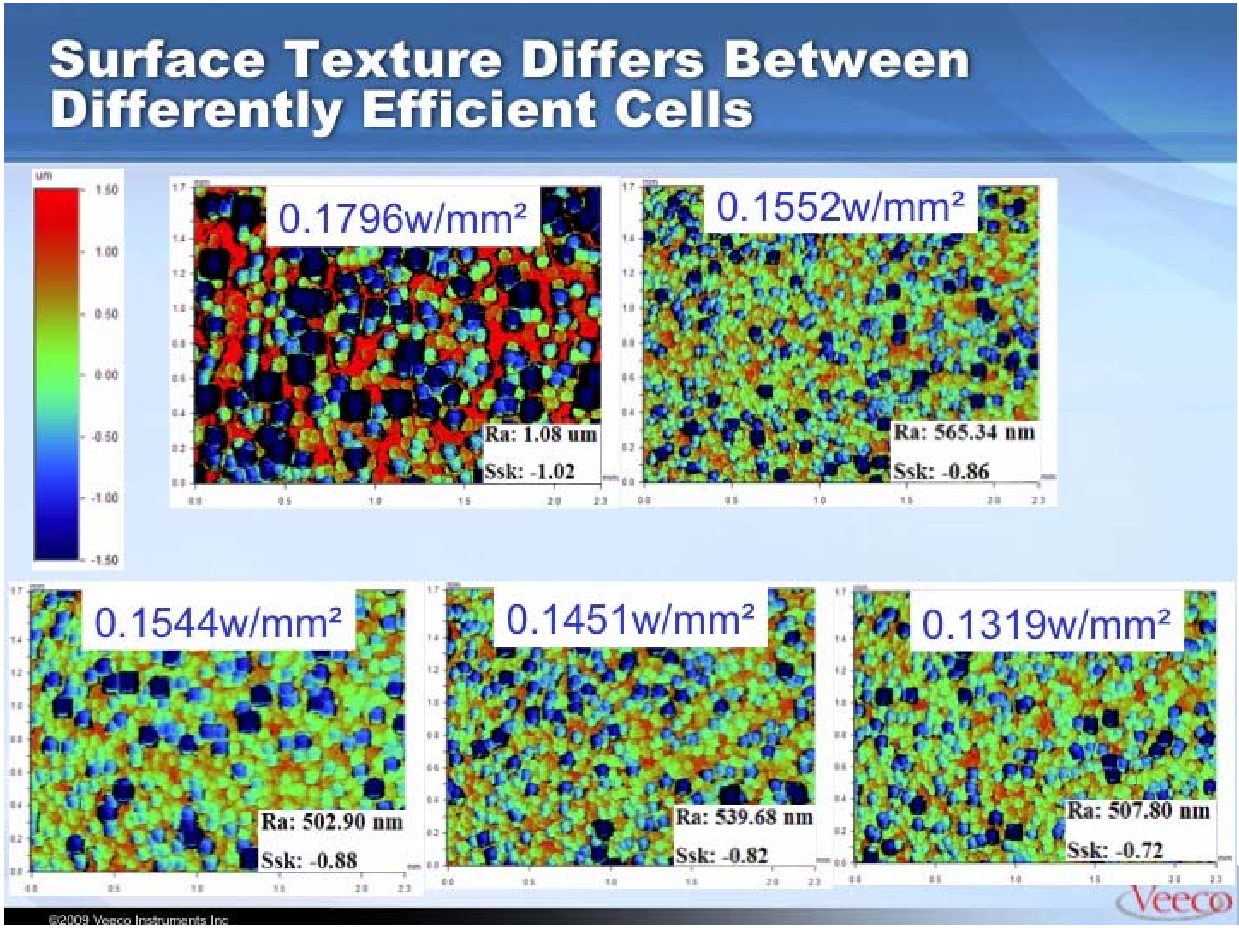

Black silicon

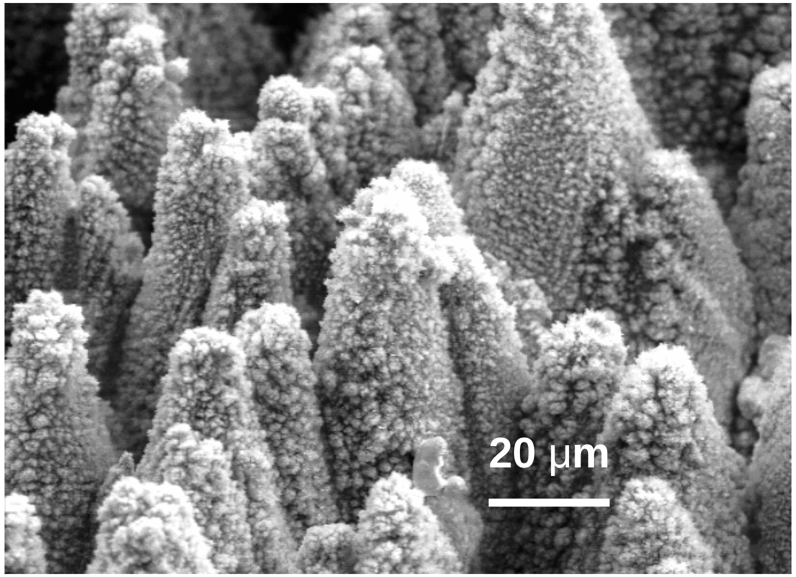

Low resolution SEM of the black silicon surface

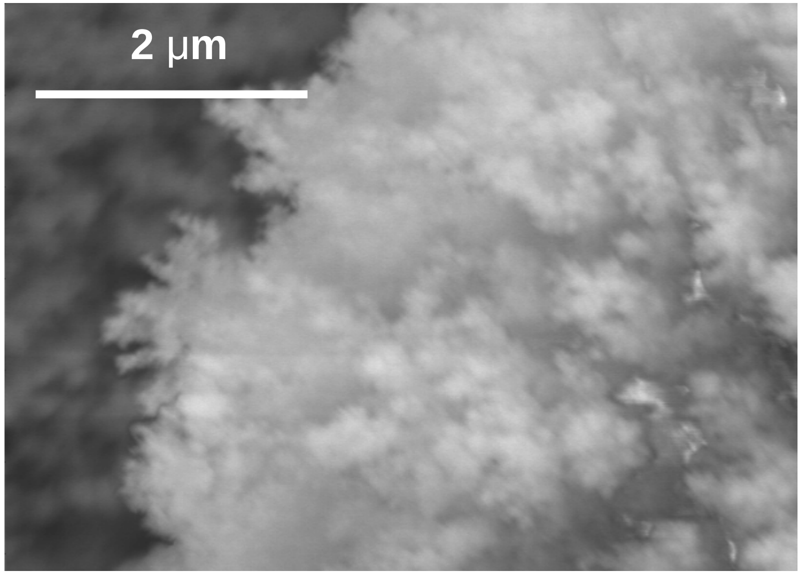

High resolution SEM of the black silicon surface

A. Serpengüzel et al., J. of Nanophotonics 2, 021770 (2008)

Black silicon samples are manufactured by shining very short (fs), very intense laser pulses at a silicon surface in air or sulfur-containing gas: air/gas reacts with the silicon surface and etches away some of it, leaving a spiked surface that is strongly light-absorbing: the surface of silicon, normally gray and shiny, turns deep black.
Non-textured silicon absorbs a moderate amount of visible light, but with a substantial reflection, while IR and UV light are transmitted or reflected with very little absorption. Spiked silicon surfaces, in contrast, absorb nearly all light at wavelengths ranging from the ultraviolet to the infrared.

Micro and nano-structuring of Si by fs laser

Halbwax et al (*Thin Solid Films 516 (2008) 6791-6795*) created a photovoltaic structure in a Si wafer by nanostructuring the surface with a fs laser before the formation of p-n junction. By optimizing the laser parameters (polarization, spot size, energy density, number of shots, scanning parameters) appropriate nanotexturization is achieved by laser treatment under vacuum (10^{-5} mbar), without SF_6.

The p-n junction is obtained by counterdoping the wafer surface by means of plasma immersion technique followed by rapid thermal annealing.

The photocurrent increases by 25-30% in the texturized areas.

Processing steps of the photocell

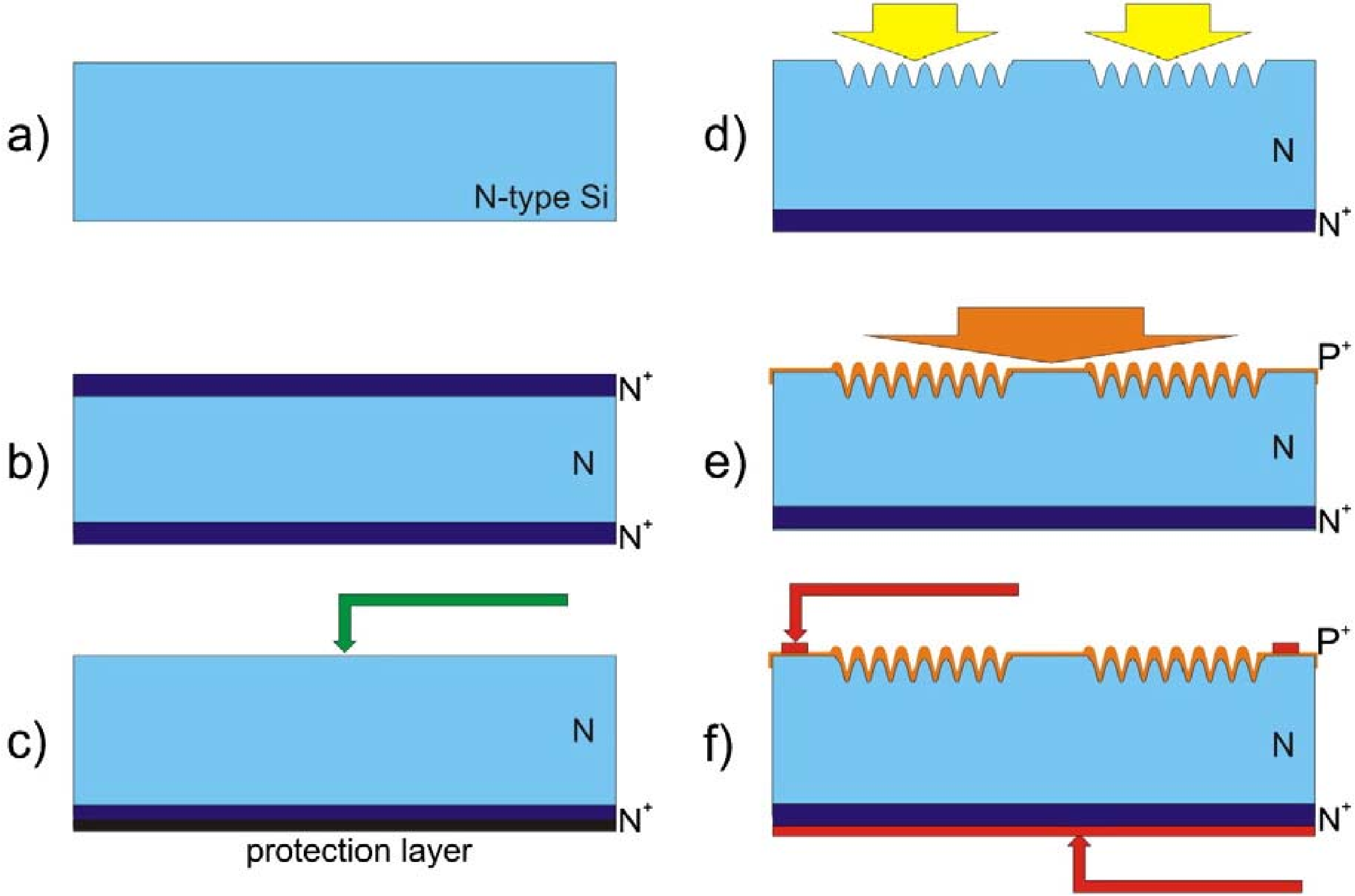

a) cleaning; b) creation of n^+ layer by diffusion; c) removal of the front n^+ layer; d) fs laser structuring; e) plasma immersion doping; f) metallization of contact

Halbwax et al (2008)

Laser processing

The engraving of Si (001) was carried out in a vacuum system with a pressure of 5×10^{-5} to 1×10^{-5} mbar. Experiments were performed using a Ti:sapphire laser (800 nm, 500 μJ energy, 1 kHz repetition rate, 100 fs pulses). Two laser fluences were used: 140 and 185 mJ/cm^2. The laser-induced structuring of the sample surfaces was produced by scanning a straight line (30 μm width) at a speed-velocity of 150 μm/s, with different d shifts (1, 2, 5 and 15 μm) between the scans to treat the whole surface and study the overlap effect.

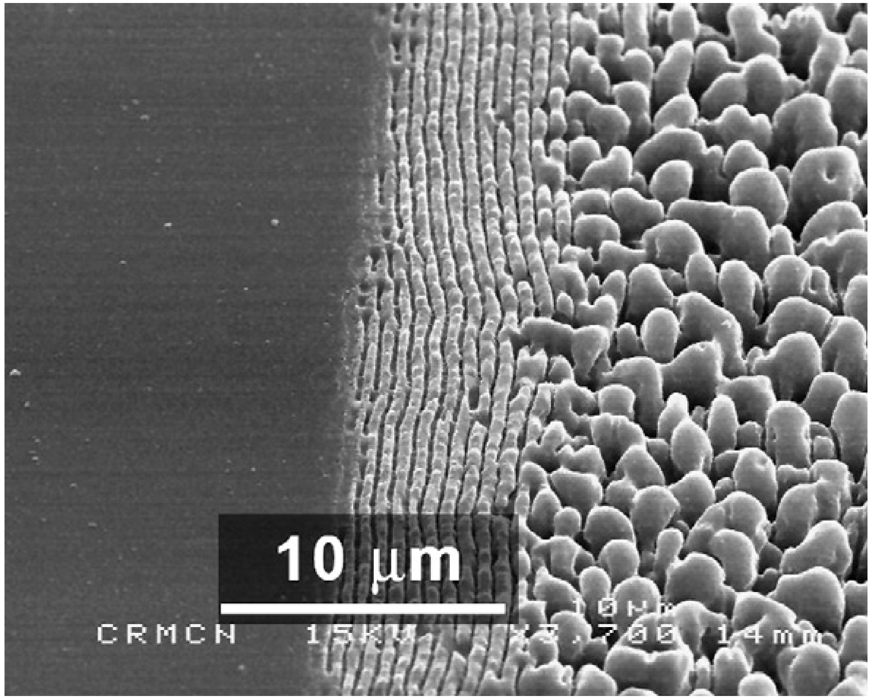

SEM photo of Laser Induced Periodic Surface Structures (LIPSS): original Si surface (left); capillary waves (periodicity 800 nm, center) and beads (about 2 μm, right). The latter are formed with higher number of pulses and energy density, since capillary waves tend to collapse and form hydrodynamically stable structures

Halbwax et al (2008)

Penguin-like structures

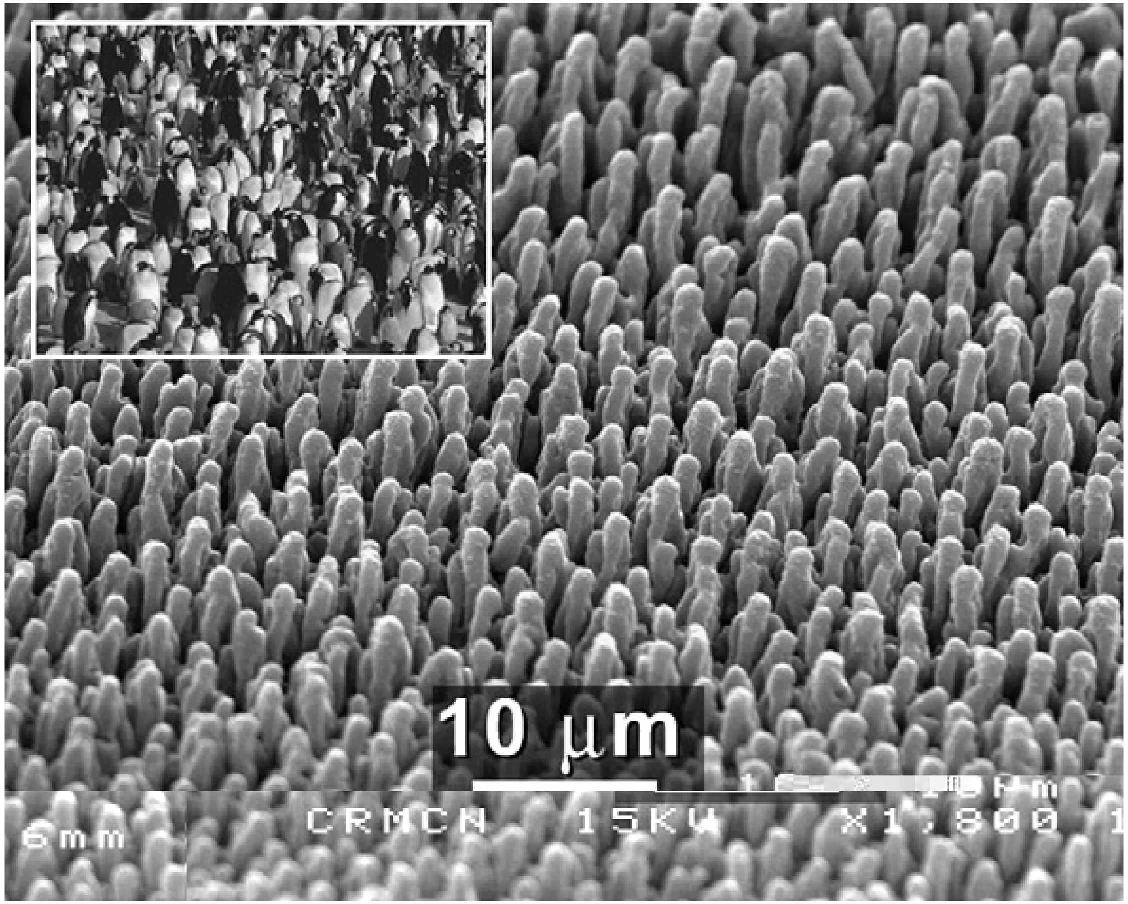

SEM photo of penguin-like structures (height approx 10 µm, spacing 2.5 µm) created by femtosecond laser (top left corner is a picture of a real penguin colony in Antartica, photo by G. DARGAUD www.gdargaud.net).

Halbwax et al (2008)

Reflectivity of nanostructured surfaces

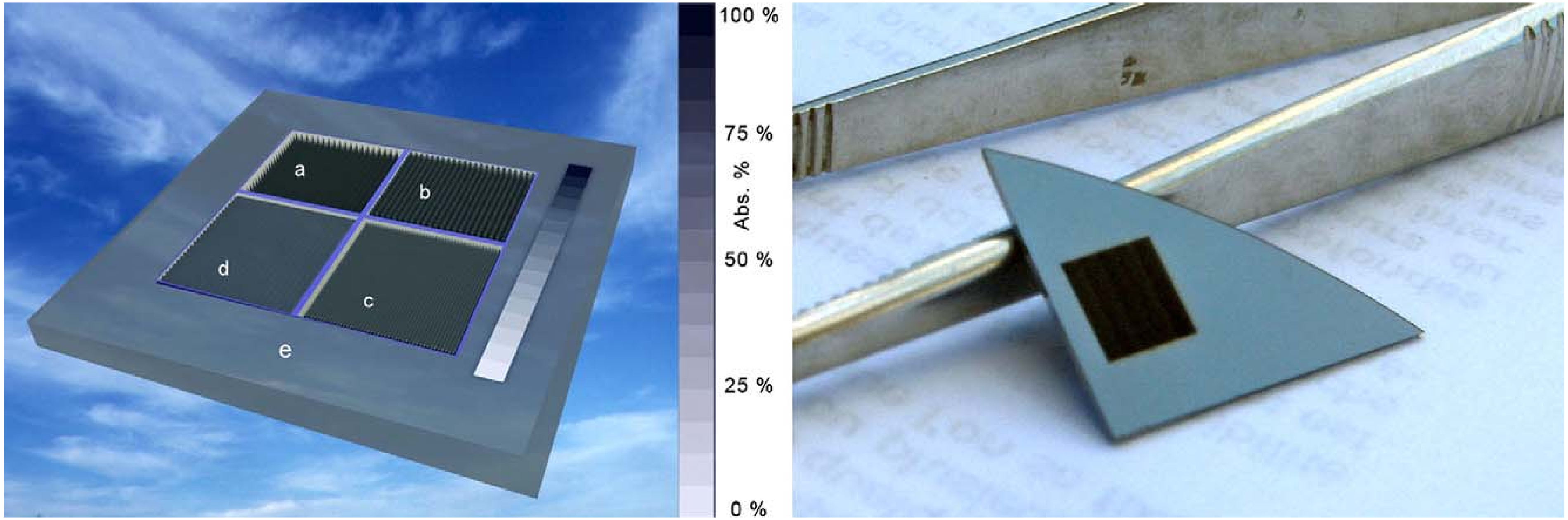

Left: 3D optical simulation of the optical absorption/reflectivity of a silicon surface with different texturizations: a) spikes b) “penguin-like” texturization c) pillars d) KOH pyramids e) flat; Right: real sample of a laser structured silicon (penguin-like).

Halbwax et al (2008)

Reflectivity of nanostructured surfaces

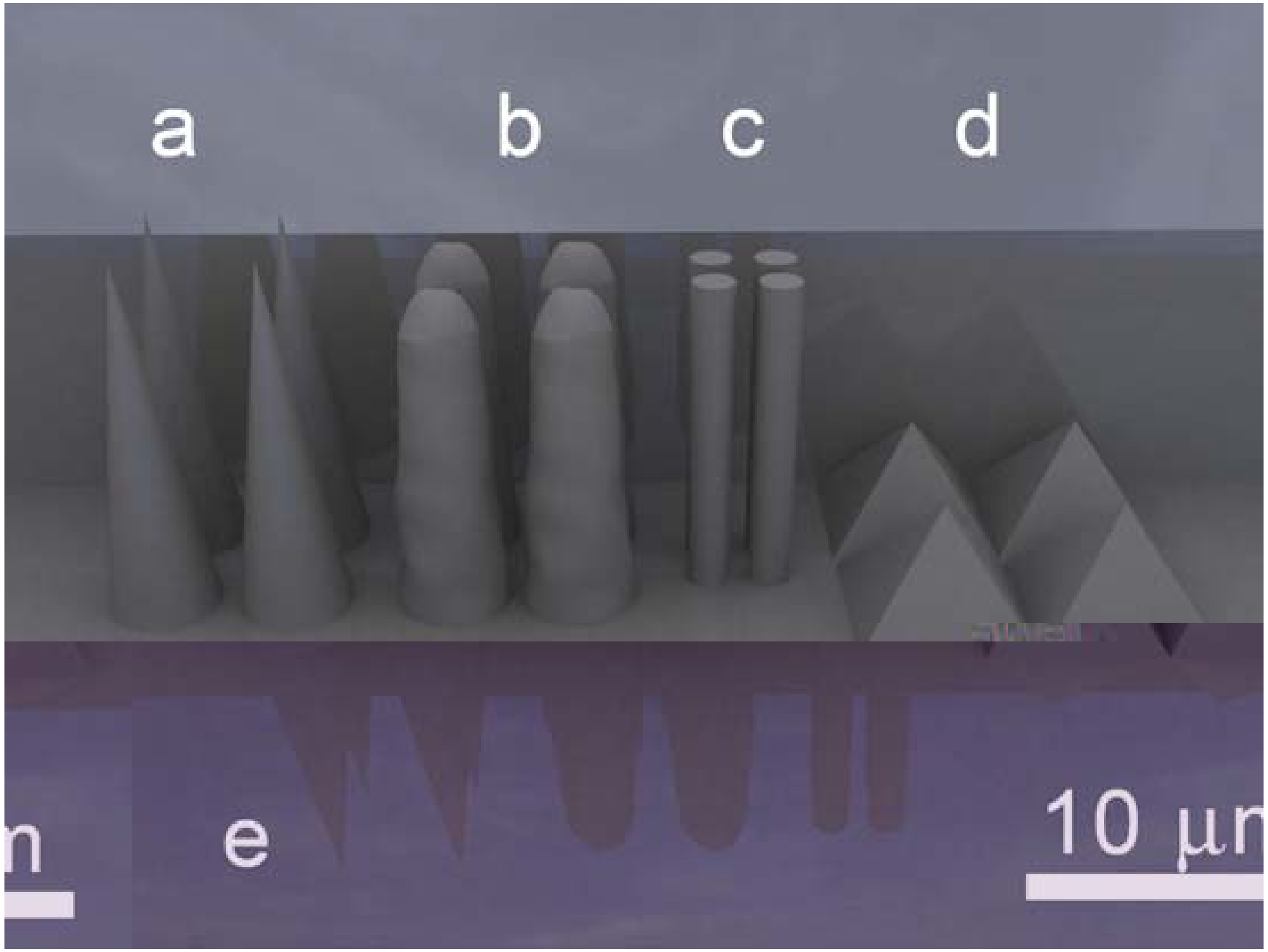

Detail of the structures used for the 3D optical simulation: a) spikes (require SF_6 gas) b) “penguin-like” texturization c) pillars d) KOH pyramids e) flat.

Halbwax et al (2008)

Reflectivity of nanostructured surfaces

Structure	Height (μm)	FWHM diameter (μm)	Spacing (μm)	Reflectiv. *R* (%) visible	Absorption *A* (%) visible
Spikes (a)	10	2.5	4	6	94
Penguin-like (b)	10	2.5	4	9	91
Pillars (c)	10	1.5	2	21	79
Pyramids (d)	5	2.5	4	27	73
Flat (e)	-	-	-	35	65

Halbwax et al (2008)

Light beam induced current scan maps

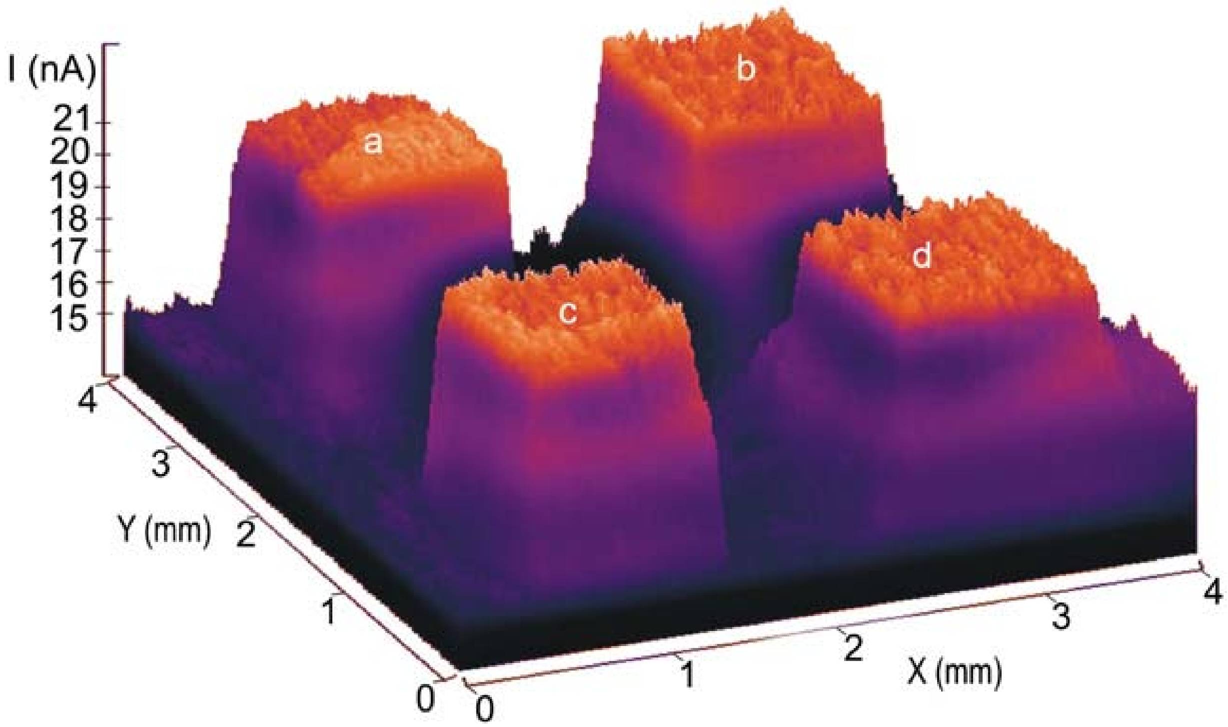

LBIC scan maps showing the increase in the photocurrent in the laser treated zones. 30 µm spot size, v=150 µm/s, a) F=140 mJ/cm^2, d=1 µm b) F=140 mJ/cm^2, d=2 µm c) F=185 mJ/cm^2, d=1 µm d) F=185 mJ/cm^2, d=2 µm.

Nanoparticle redeposition

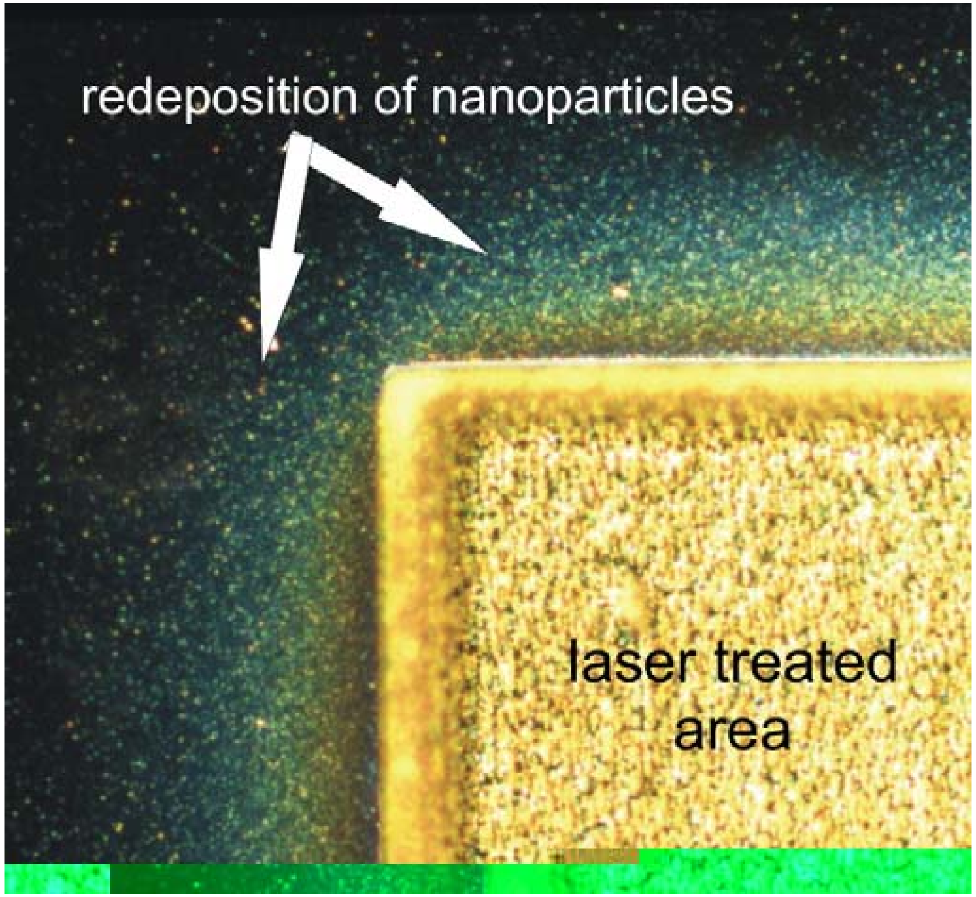

Optical microscope view (dark field) of a laser treated area (F=185 mJ/cm^2, v=150 μm/s) showing the nanoparticle redeposition outside the spot: increased absorption.

Halbwax et al (2008)

Conclusions

- Laser micro and nanostructured Si structures exhibit reduced reflection and high absorption (black silicon)
- Absorption increase also around the laser-treated area due to nanoparticle redeposition
- Photocurrent increase in the laser-treated areas
- Promising samples were obtained in void, with no use of SF_6, identified by the Kyoto Protocol as one of the main greenhouse gas that contribute to climate change and global warming